Logical Superposition Coded Modulation for Wireless Video Multicasting

by

James Ching-Chih Ho

A thesis
presented to the University of Waterloo
in fulfillment of the
thesis requirement for the degree of
Master of Applied Science
in
Electrical and Computer Engineering

Waterloo, Ontario, Canada, 2009

I hereby declare that I am the sole author of this thesis. This is a true copy of the thesis, including any required final revisions, as accepted by my examiners.

I understand that my thesis may be made electronically available to the public.

Abstract

This thesis documents the design of logical superposition coded (SPC) modulation for implementation in wireless video multicast systems, to tackle the issues caused by multi-user channel diversity, one of the legacy problems due to the nature of wireless video multicasting. The framework generates a logical SPC modulated signal by mapping successively refinable information bits into a single signal constellation with modifications in the MAC-layer software. The transmitted logical SPC signals not only manipulatively mimic SPC signals generated by the superposition of multiple modulated signals in the conventional hardware-based SPC modulation, but also yield comparable performance gains when provided with the knowledge of information bits dependencies and receiver channel distributions. At the receiving end, the proposed approach only requires simple modifications in the MAC layer software, which demonstrates full decoding compatibility with the conventional multi-stage signal-interference cancellation (SIC) approach involving additional hardware devices. Generalized formulations for symbol error rate (SER) are derived for performance evaluations and comparisons with the conventional hardware-based approach.

Acknowledgements

Since starting at the University of Waterloo, many of my lifelong lessons were taught by individuals who are probably unaware of their impressions on me over the years.

I express the deepest appreciation and gratitude to Professor Pin-Han Ho, who has provided his exceptional insight and consultation in the development of my research interests. He has positively influenced me in many ways and has always been available for both social and academic counsel throughout my undergraduate and graduate years.

I would like to acknowledge James She, who has been invaluable as a research partner and friend. This thesis is based upon our joint research, and only with his dedication, wisdom, and inspiration, could I have completed everything on time.

Thank you Professor Bill Bishop and Professor Guang Gong for reading my thesis and attending my seminar milestone under such short notice (once again!) and of course, for your insights.

Finally, I would like to thank: the guys, Jaimal, Tariq, Alan, and Dan, for keeping me sane; Kevin for illustrating the outrageousness in life; Tracy for baiting me with the exciting times to come; Jennifer for her friendship from afar; most importantly, my brother, Jason, for being my role model.

Thank you Christie for showing me the sweetness of living life.

Thank you everyone for your belief in me.

For the most loving Father and Mother, who sacrificed all for our destinies.

Contents

List of Tables

List of Figures

Chapter 1

Introduction

Advancements in 3G and 4G Wireless Broadband Access (WBA) technologies based on Long Term Evolution (LTE) and IEEE 802.16 (WiMAX) standards, as well as the scalable video coding technologies, such as H.264/MPEG4 Advanced Video Coding (AVC), have enabled the provisioning of large-scale wireless video multicast and broadcast services, such as mobile Internet Protocol Television (IPTV) and wireless digital signage. Adopting video multicasting achieves the best scalable usage of transmission capacity at the base stations (BSs), where system scalability becomes dependent only on the desired number of simultaneously provisioned television channels and their specific bandwidth requirements instead of the number of receivers. This facilitates the largest scale and highest quality wireless broadcasting for video data such as scheduled and live television content, in which multiple receivers simultaneously receive the bandwidth-intensive data of the same video stream.

1.1 Addressing Multi-User Channel Diversity

One of the legacy problems in the aforementioned applications is due to multi-user channel diversity, where the selection of a proper multicast transmission rate for the intended receivers at each time moment becomes a challenging issue. A single choice for modulation results in mono-rate multicast signals, which can be simultaneously considered both too conservative and too aggressive depending on the channel conditions of specific receivers. The lack of resolution in the mono-rate signal results in a choice of modulation that can only be catered to a specific type of channel condition, failing to address the needs of receivers with channel conditions not optimized for the choice of modulation. As a result,

receivers with poor channel conditions may not be able to decode any portion of a video broadcast, while other receivers with better channel conditions may have under-utilized channel capacities. To maintain service continuity to all receivers, a straightforward rigid solution could be implemented such that the most conservative transmission rate is adopted to satisfy the receiver with the worst channel condition. This approach allows all intended receivers to maintain a constant robust rate, however, at the expense of the reduced amount and quality of video channels that can be jointly provisioned, which leads to poor economic scalability.

Superposition coded (SPC) modulation is a physical-layer technique enabled by hardware circuitry that allows a transmitter to send individual information to multiple receivers simultaneously within a single wireless broadcast signal [1, 2]. A SPC signal contains a multi-resolution modulated symbol, enabling a receiver to decode its own, as well as its peers' information if its channel condition is sufficient for the higher resolution. Creatively, the multi-resolution nature of SPC signals has been exploited for the use of transmitting scalable video streams, which themselves are multi-resolution encoded. The scalable video streams are encoded into multiple quality layers, and in [3-9], SPC is studied and employed into a cross-layer design that generates wireless multicast signals for the transmission of such video streams. Those studies show that SPC multicast can effectively resolve the multi-user channel diversity problem, where the generated multi-resolution modulated signals can perfectly scale to the wireless multicasting or broadcasting of successively refinable information, such as scalable video bit streams. It has been demonstrated that by superimposing multiple video quality layers into a single SPC modulated signal, receivers with poor channels can decode and obtain the base layer data to maintain a basic video perceptual quality. On the other hand, receivers with good channel conditions may obtain, in addition to the base layer, the data of higher quality layers, which refines the data of lower layers such that an improved video quality is perceived.

In spite of the aforementioned advantages, very few commercially available wireless systems and industry standards for wireless video multicast have defined or supported SPC modulation. The absence of SPC modulation in wireless video multicast applications is likely due to the requirement of additional system support, in which dedicated hardware components and circuitry are necessary to superimpose two or multiple modulated signals together to form a SPC signal in the physical (PHY) layer. Also, software modifications

are required to enable the cross-layer mapping between the successively refinable video sources and the layered SPC multicast signals. In the present and past, such additions of dedicated hardware and software support could not be justified in current and past wireless systems, mainly due to the lack of broadband digital media applications on video multicasting subscriptions. However, by envisioning the prevalence of bandwidth-intensive video multicasting services provisioned using emerging WBA networks, it is becoming crucial to develop a practical implementation of SPC modulation for wireless video multicasting that offer minimal barriers to industry acceptance.

Motivated by these observations, this thesis introduces a novel cross-layer design framework, known as logical superposition coded (L-SPC) modulation, for the multicasting of successively refinable information such as scalable video bit streams, aiming to mitigate the vicious effect of multi-user channel diversity, a legacy problem that needs to be immediately addressed in practical implementations of scalable wireless video multicasting in modern WBA networks.

1.2 Thesis Contributions

The proposed framework is characterized by a number of contributions, which tackle a number of issues outlined in the previous section.

One of the major barriers for conventional SPC (C-SPC) adoption is the requirement of dedicated hardware components and circuitry to superimpose two or multiple modulated signals in forming a SPC signal. Such hardware constraints are also present in the receiver. The proposed logical approach addresses such issue in a way that additional hardware in existing wireless systems and standards are not necessary. Specifically, the proposed logical process involves a strategic mapping of refinable information bits of base and enhancement quality layers from a scalable video bit stream into a logical SPC signal, using the functions of dynamic power allocation and phase shift assignment commonly available in modern communication chipset designs from companies such as picoChip Inc., UK and Wavesat Inc., Canada. At the receiving end, instead of using a dedicated SPC demodulator, the subscriber only needs to decode the received logical SPC modulated signals using industry standard demodulators. In summary, the hardware constraints for

SPC implementation has been removed and replaced with only necessary software modifications in the MAC layer, which can be performed through driver or firmware installation procedures. Compatibility is also ensured since the L-SPC transmitter has the capability to mimic symbols generated using conventional SPC modulation from any combinations of QAM modulated signals adopted in current and emerging wireless standards.

Through extensive simulations, results from the performance evaluation of L-SPC demonstrate that the proposed logical SPC approach can achieve equivalent performance in terms of the overall system throughput, in comparison to the conventional hardware-based SPC implementation. In achieving comparable performance, along with the advantages from reduced implementation complexity, the single barrier blocking SPC from mass industry acceptance has been removed. Thus, L-SPC is the proposed superposition coding implementation with potential for industry acceptability and market deployment. In this sense, the proposed cross-layer framework for logical SPC video multicast is expected to solidly improve the required economic scale of wireless video multicast systems in emerging WBA networks.

The thesis organized as follows. Chapter 2 provides a background on the SPC technique and its interplay with scalable video bit streams in wireless multicasting. In Chapter 3, the cross-layer design of the proposed logical SPC modulation is introduced. Derived generalized formulations applicable to any combination choice of two-layered SPC symbols are presented in Chapter 4. In Chapter 5, performance evaluation is conducted and the results are presented. Chapter 6 provides the conclusive remarks which summarize the contributions of this research topic.

Chapter 2

Background

Without loss of generality, the thesis will begin with the presentation of the proposed video multicast framework through a case study using two-layered scalable video sources interplayed with a two-level SPC modulation employing the BPSK and QPSK modulation schemes. The two layers of scalable video are known as the base and enhancement layers, where a dependency exists between the two layers. Note that the proposed technology is applicable to a successive refinable source with any number of quality layers, corresponding to the same number of levels in the SPC modulation employing any arbitrary combinations of modulation schemes.

2.1 Superposition Coding

The intrinsic goal of SPC is to facilitate the transmission of two independent receiver's information in a single wireless transmission block by the superimposition of the two signal's symbol blocks. The superposition of two signals is analogous to the vector addition of the signal constellation symbols. As shown in Fig. 2.1, x_1 and x_2, are information for receiver 1 modulated using QPSK and information for receiver 2 modulated using BPSK, respectively. Modulation using QPSK has the capability to achieve a higher transmission rate over BPSK at the expense of robustness when subject to a noisy channel. The superimposed signal, x, is a vector sum of the two modulated signals governed by $x = x_1 + x_2$. In Fig. 2.1(c), vector x consists of symbol '0' from Fig. 2.1(b) and symbol '01' from Fig. 2.1(a). Signal x is the SPC symbol, launched as a single wireless transmission block, received by two receivers with diverse channel conditions within the same coverage.

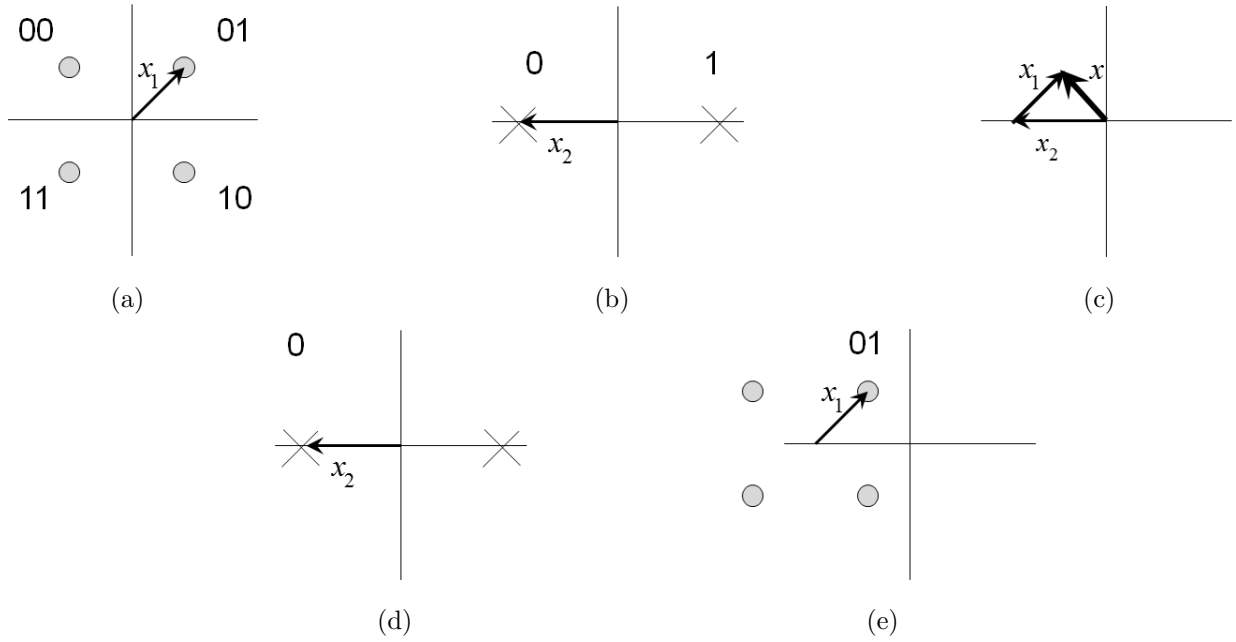

Figure 2.1: Superposition coded (SPC) modulation: (a)-(c) encoding; (d)-(e) decoding [7].

The received signal is expressed as $y_j = x + z_j$, where z_j is the noise perceived by receiver j. The conventional technique to decode the received SPC signals is known as Signal-Interference Cancellation (SIC), which is used at receiver j to identify the signal components meant for the noise and other receivers. Thus, receiver j can obtain its own information by subtracting the undesired signal components belonging to other receivers from its received signal y_j. For example, for receiver 1 to decode its data from y_1, it must first use the demodulator corresponding to the information used for receiver 2, x_2, and then use SIC to subtract x_2 from the received signal y_1. The result of the subtraction using SIC is x_1, which is usually distorted by the noise experienced at receiver 1, z_1.

2.2 Related Research

A two-level SPC multicast (SCM) was proposed in [3-7] for the multicasting of scalable video over a wireless link to provision scheduled IPTV services. Instead of using a single modulation scheme for each multicast transmission each time, the studies suggested assigning successively refinable data from a scalable video source to layered SCM signals at the channel. Specifically, each multicast signal is generated at the channel by superimpos-

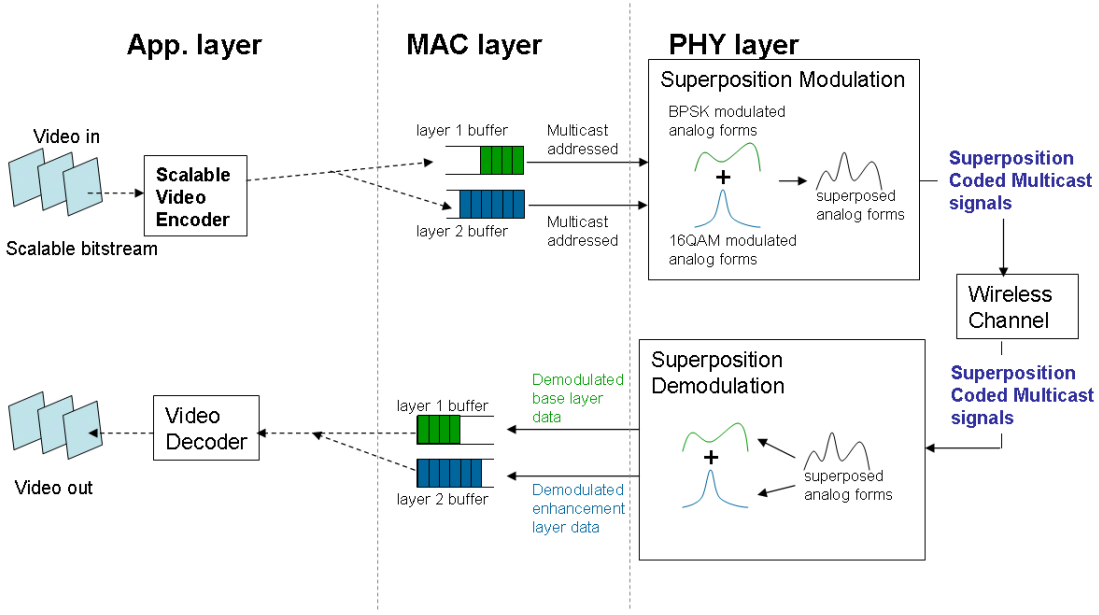

Figure 2.2: Schematic diagram of superposition coded multicast for successively refinable video source [7].

ing some video data from the base quality layer, modulated by a lower-order modulation such as BPSK, as well as some video data from the enhancement quality layer, modulated by a higher-order modulation such as QPSK. Thus, a receiver can either obtain the base video quality of an IPTV channel by partially decoding the multicast signal for those bit streams modulated using BPSK under poor channel conditions, or obtain the full video quality modulated by both BPSK and QPSK by successfully decoding the whole SCM signal under good channel conditions. The scheme effectively overcomes the vicious effect due to multi-user channel diversity and solidly improves the system throughput for better economic scalability in provisioning video multicasting services. It can also eliminate service disruptions, at moments of poor channel conditions experienced by certain receivers, by preserving the base video quality during those instances. A schematic diagram of SCM for a successively refinable video source is shown in Fig. 2.2.

All previous studies have assumed the adoption of a hardware-based SPC implementation for both the modulator and demodulator, to support the superposition of two modulated signals at the transmitter and the Signal-Interference Cancellation process used by all receivers. There has not been any logical mapping mechanism developed for wireless video multicasting using a suite of software-defined SPC modulation and demodulation

procedures. These issues overshadow the demonstrated advantages of using SCM to address the legacy issue of multi-user channel diversity and have posed a fundamental barrier from its implementation into modern wireless communication systems for video multicast.

Chapter 3

Logical Superposition Coding

This chapter presents the designs of the proposed logical SPC modulation and demodulation scheme, which incorporates a cross-layer design framework for wireless video multicasting. The transmitter design in generating logical SPC multicast signals is first discussed, followed by the corresponding design at the receivers, which demodulate the SPC multicast signals to retrieve the scalable video bit stream.

3.1 Transmitter Design

The goal of the L-SPC transmitter is to perfectly mimic SPC symbols generated using the hardware-based C-SPC. For conceptual demonstration, this chapter considers a case study where an SPC modulated signal contains information bits of two-layered scalable video bit streams. In the example shown in Fig. 2.1, a superimposed signal x can be taken as the summation of the two vectors expressed in terms of the corresponding amplitudes and phases in a constellation diagram, formed by the conventional approach using the BPSK and QPSK modulation schemes. The resultant constellation diagram of signal x consists of eight possible symbols, each with a unique combination of amplitude and phase. The amplitude and angle of each resultant SPC symbol depends on the allocation ratio of energies in each transmission for BPSK and QPSK modulated signals in the conventional approach, denoted by E_1 and E_2, respectively. There is a total energy constraint, where the total energy available to all layers must remain constant in each broadcast transmission, with β as the single parameter governing the relationship between E_1 and E_2:

$$E = E_1 + E_2; \tag{3.1}$$

$$E_1 = \beta E; \tag{3.2}$$

$$E_2 = (1 - \beta)E. \tag{3.3}$$

3.1.1 One-Shot Modulator

The unique representation of the resultant SPC constellation diagram using corresponding amplitudes and phases translates into an observation that such superimposed signal can be directly generated in *one-shot* at the transmitter through dynamic phase shift keying and power allocation to manipulate the respective angle and amplitude of x in the SPC constellation diagram.

By identifying the required number of constellation points and manipulating the value of β from Eqs. (3.2)-(3.3), the proposed logical SPC modulation can generate an eight-point constellation diagram identical to the resultant constellation generated by the conventional hardware-based SPC. Generalizing the concept of one-shot modulation at the transmitter, L-SPC can be generically used to produce SPC multicast signals equivalent to any combination of common modulation schemes. In Table 3.1, the total number of points in the SPC constellation diagram can be identified given any choice of modulation scheme combinations for the base (Layer 1) and enhancement (Layer 2) layers. As a result, the conventional process used in C-SPC for the superposition of two modulation signals can be simplified to a one-shot modulator requiring only the amplitude and phase of each resultant SPC symbol. For the case study in this chapter, instead of the super-

Table 3.1: Equivalent number of constellation symbols for various two-layered modulation choices.

Layer 2 \ Layer 1	BPSK	QPSK	16-QAM
QPSK	8	-	-
16-QAM	32	64	-
64-QAM	128	256	1024

position of the BPSK-modulated base layer and QPSK-modulated enhancement layer, the eight-symbol SPC constellation can be generated in one-shot. The generated one-shot constellation symbols can be configured for amplitudes and phases equal to those generated

by a conventional hardware-based SPC approach. Note that the mapping of information bits using both conventional and logical SPC generation approaches must be identical for both methods to be logically equivalent.

3.1.2 Cross-Layer Mapping

To realize the proposed logical SPC modulation for video multicast, strategic mapping of the $\log_2 m_1$ bits from the base layer and $\log_2 m_2$ bits from the enhancement layer is required into a $(\log_2 m_1 m_2)$-bit symbol block. Referring back to the case study, each symbol block contains one bit from the base layer and two bits from the enhancement layer, corresponding to the number of bits in the respective BPSK and QPSK symbol. The upper portion of Fig. 3.1 illustrates the superposition of two conventional modulation schemes to yield the resultant constellation diagram with eight points, as shown in the lower portion of Fig. 3.1, mapped from the 3-bit symbol block.

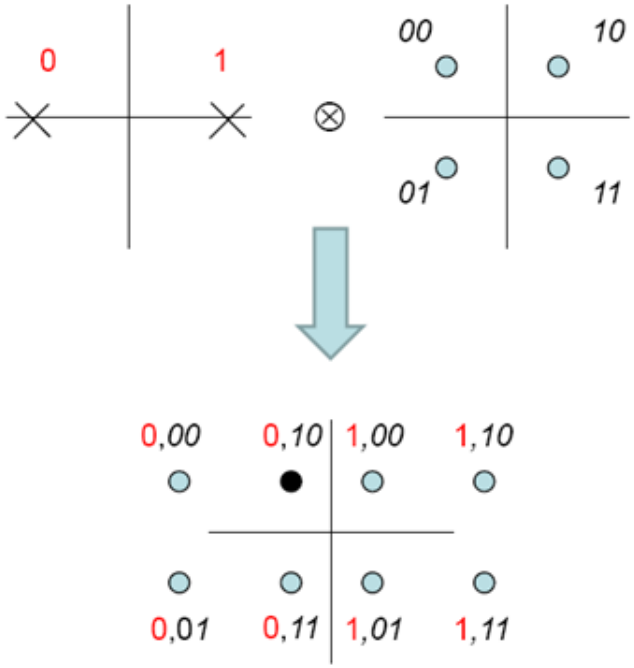

Figure 3.1: Mapping of a 3-bit symbol block to one of the eight constellation symbols [7].

The mapping of the 3-bit symbol block to the 8-point constellation is based on the knowledge regarding the information bits of the scalable video bit streams in the application layer. For a symbol referring to '0' in the base layer and a symbol referring to '01' in the

enhancement layer, a corresponding 3-bit symbol block containing '001' (i.e. '0' | '01') can be formed and mapped to the symbol '0, 01' in the *one-shot* constellation diagram of the existing modulation scheme for generating a logical SPC modulated signal equivalent to the conventional approach.

3.1.3 Transmitter Software Support

The implementation of logical SPC modulation at the transmitter requires a new software module in the existing MAC layer to obtain the knowledge of information bits dependency between the two quality layers from the scalable video source. Data from different layers are buffered in the corresponding queues at the transmitter. The modified MAC software interacts with the modulation chipset in the PHY layer through a set of primitives to execute one-shot modulation to generate logical SPC multicast signals, as shown in Fig. 3.2.

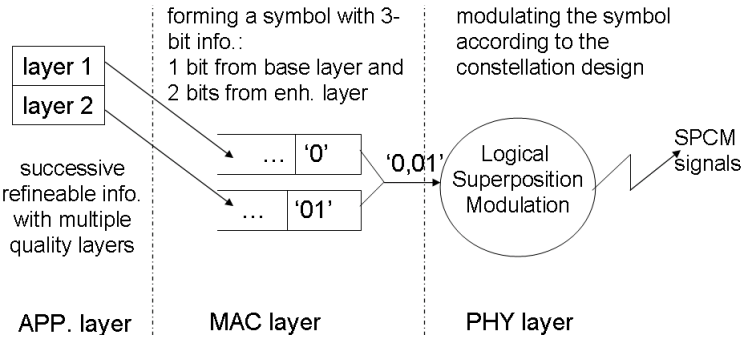

Figure 3.2: Software support required for interactions between architectural layers at the transmitter [7].

The primitives facilitating the interaction between the modified MAC and PHY layers act as a passage for the MAC software to define the *one-shot* modulation scheme in the PHY layer. The interaction selects a constellation point to map the set of bits at the head-of-line of the corresponding queues to a 3-bit symbol block. In the modulation chipset, on the other hand, more functions should be added such that some service access points (SAPs) are defined in order to receive and recognize the parameters passed from the upper MAC software. The chipset should also be able to generate the logical SPC modulated signals accordingly, based on the energy allocated for each modulation layer.

Note that the symbol locations in the SPC constellation diagram can be dynamically determined by the given amplitude and phase for each symbol through the control of β, which, in turn, affects the transmission performance required for the application in terms of the symbol error rate (SER) or overall symbol throughput.

Since variable energy allocation and dynamic phase keying assignment are becoming common functionalities in modern wireless chipsets, the aforementioned software modifications would not introduce much overhead in the state-of-the-art base station system. Therefore, the proposed logical SPC modulation scheme is feasible and implementable in currently available commercial base station systems.

3.2 Receiver Design

In an effort to remove the hardware modification constraints necessary in the process of conventional SPC demodulation, L-SPC leverages existing receiver demodulators to eliminate the signal-to-interference cancellation process and hence, removes the corresponding hardware modifications needed to demodulate SPC signals.

3.2.1 One-Shot Demodulator

Continuing with the case study introduced in this chapter, the proposed logical SPC demodulation allows the direct decoding of both base and enhancement layer information by the use of a standard 8-QAM demodulator. Such approach is in contrast to the hardware-based SPC demodulation requiring SIC.

In regards to the base layer information, for example, the first bit of a symbol block in Fig. 3.1, carrying the base layer information, can always be obtained as '0' as long as the received logical SPC signal is interpreted as any point on the left-hand-side of the constellation diagram. This is due to the strategic mapping of information bits of each symbol block to a constellation point, as shown in Fig. 3.1. Intuitively as a result to such strategic mapping, the logical one-shot approach achieves equal base layer symbol error in comparison to the conventional SIC approach. Thus, the one-shot standard 8-QAM demodulator employed in L-SPC incorporates the base layer detection process and thus,

effectively eliminates the first stage of C-SPC, where a BPSK demodulator is used to decode the base layer information. In regards to the enhancement layer information, instead of subtracting the detected base layer bit for the decoding of the enhancement layer bits using SIC, the enhancement layer has already been decoded during the one-shot demodulation process employed in L-SPC.

In summary, the logical SPC receiver simultaneously recovers both base and enhancement layer information using the *one-shot* demodulator, simplifying the SPC symbol detection process while eliminating the hardware requirement constraints present in the conventional SPC demodulator. Since no hardware subtraction is required, the received logical SPC modulated signals can be decoded using an existing demodulator already implemented in commercially available hardware chipsets. However, additional software support is needed to retrieve the original video bit stream for playback, which is discussed in the next subsection.

3.2.2 Receiver Software Support

The proposed software support for logical SPC demodulation at the receiving end is designed for simple implementation with easy installation and minimal overhead. Such design requirements are crucial for low-cost, mass-produced devices used in customer premise equipments (CPE).

To demodulate logical SPC multicast signals using the proposed implementation, the receiver only requires knowledge of the two modulation schemes employed for the SPC signal at the transmitter. With such knowledge and letting the result from the one-shot 8-QAM demodulation be $a_1b_2b_3$, the application layer categorizes the first bit, a_1, as part of the base layer bit stream and the remaining two bits, b_2b_3 as part of the enhancement layer bit stream. Since a_1 is the most important bit, it is modulated using the more robust BPSK modulation scheme such that the base video quality is more likely to be secured. Furthermore, a better perceived video quality can be achieved if the two enhancement layer bits from the QPSK modulation portion of the SPC symbol, b_2b_3, are successfully decoded.

The aforementioned design incurs very limited additional signalling and software modifications. Minimal additional signalling is necessary since the transmitter and receivers only need to establish choices for two modulation schemes based on pre-defined algorithms.

Minor software modifications in the MAC layer are needed to split each obtained symbol into two portions, where the bits of the first part are assigned to the buffer for the base layer and the bits remaining are assigned to the buffer for the enhancement layer. Finally, only one additional mechanism is required within the video decoder used by receivers in the application layer to extract the bits from both queues for reconstruction of the original video bit stream.

In comparing L-SPC with the conventional SIC-based demodulation process, both schemes need separated buffers and interfaces to handle the individual streams of information bits from the multi-stage decoding processes. However, the modified software in the proposed scheme yields all information bits from a single demodulation process in *one-shot*, and then assigns the first $\log_2 m_1$ bits and subsequent $\log_2 m_2$ bits into respective buffers of the base and enhancement quality layers, which is a relatively straightforward procedure.

3.3 Design Operational Range

Traditionally, the decision regions in a constellation diagram places individual symbols equidistantly apart to achieve optimal symbol error probability. The requirement of equidistance is based on the assumption of equal importance of each encoded bit in a symbol block. However, this is not necessarily a desirable feature when transmitting successively refinable bit streams using SPC modulation, due to the dependency of information bits between successive layers, and scalability issues in the presence of multi-user channel diversity. When SPC is used, the energy allocation parameter, β, can be manipulated to optimally place each constellation symbol for maximized perceived video quality.

The novel concept of using a *one-shot* demodulator in the receiver design of L-SPC places bounds on β for a standard demodulator to be feasibly applied to demodulate the proposed logical SPC signal. This section continues the case study, basing the explanations and derivations of the bounds on the superposition of BPSK and QPSK signals, where a constellation with eight points is yielded, to determine the feasible operational range of β when decoding using the proposed L-SPC demodulator. The operational range of β is bounded by $\beta_{\min}$ and $\beta_{\max}$ such that the β range of interest is

$$\beta_{\min} < \beta < \beta_{\max}. \tag{3.4}$$

The use of a standard 8-QAM demodulator at the receiving end instead of a specialized demodulator for SPC demodulation bears many advantages for implementation and industry acceptance, which is one of unique features of the proposed cross-layer design. The necessary condition to feasibly use a standard 8-QAM demodulator is that any one of the eight SPC constellation points must be positioned within the correct decision regions understood by a standard 8-QAM detector. This places constraints on the energy allocation parameter β, which determines the resultant locations of the constellation points.

Let a logical SPC modulated signal be generated according to Eqs. (3.2)-(3.3), which is equivalent to the superposition of two BPSK and QPSK signals with E_1 and E_2 as the corresponding energies. The resultant constellation diagram has eight constellation points, as shown in Fig. 3.3. The lower and upper bounds on β are derived by identifying situations where any one of the eight points in the SPC constellation occurs outside the correct decision boundaries of a standard 8-QAM demodulator when the noise power is zero.

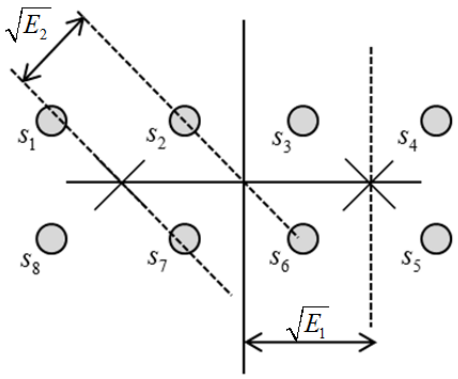

Figure 3.3: Case study SPC constellation diagram.

3.3.1 Lower Bound on β

Based on definitions in Eqs. (3.2)-(3.3), decreasing β is equivalent to allocating more energy for the enhancement layer information. This action causes the locations of the four points s_3, s_4, s_5, and s_6 to move further away from each other, while their centre, marked $\times$ in Fig. 3.4, moves closer to the origin. The decrease in β reduces $\sqrt{E_1}$ and increases $\sqrt{E_2}$. The lower bound of interest occurs when the horizontal component of $\sqrt{E_2}$ becomes equal to $\sqrt{E_1}$. Thus, $\beta_{\min}$ is defined as the lower bound which occurs when Eq. (3.5) is

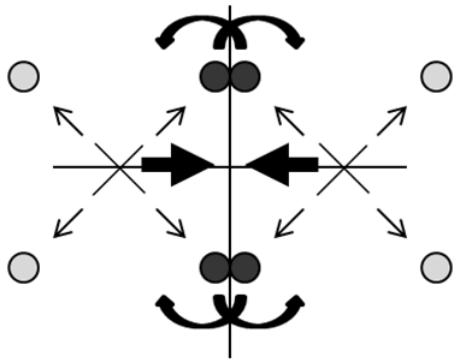

Figure 3.4: Decreasing β with arrows showing directions of symbol movement.

satisfied.

$$\sqrt{E_1} = \sqrt{E_2}\cos 45^{\circ} \tag{3.5}$$

Substituting Eqs. (3.2)-(3.3) into Eq. (3.5) and solving for $\beta_{\min}$,

$$\sqrt{\beta_{\min} E} = \frac{1}{\sqrt{2}}\sqrt{(1-\beta_{\min})E}, \tag{3.6}$$

$$\beta_{\min} = \frac{1}{2}(1-\beta_{\min}), \tag{3.7}$$

$$\beta_{\min} = \frac{1}{3}. \tag{3.8}$$

Referring back to Fig. 3.3, if the power allocation parameter is set to $\beta_{\min}$, s_3 and s_2 are overlapping along the vertical axis. If β is further decreased, even when there is no noise, s_3 and s_2 becomes located outside of their correct standard 8-QAM decision regions. As a result, persistent errors occur for these two symbols when a standard one-shot 8-QAM demodulator is used for decoding. Due to symmetry, the same behaviour occurs to the movements of s_1, s_2, s_7, and s_8 from variations in β with the same condition causing s_7 to overlap with s_6.

3.3.2 Upper Bound on β

Since L-SPC uses a one-shot demodulator, the decision regions used to determine the received symbol is based on the standard 8-QAM decoder, where equidistant symbol placement is assumed. Thus, standard 8-QAM decision boundaries constrain the upper ranges of β. To determine the location of the standard 8-QAM decision boundary, note that the vertical boundary along the positive abscissa corresponds to the location of the base layer

symbol, marked $\times$ in Fig. 3.3. Thus, this boundary is located at $\sqrt{E_1}$ when β is set to β_{eq} for an equidistant constellation. Equidistance occurs when the amplitudes of the base layer constellation symbols are equal to the horizontal distance between enhancement layer symbols. Thus, the condition on $\sqrt{E_1}$ and $\sqrt{E_2}$ for equidistance is given by Eq. (3.9).

$$\sqrt{E_1} = 2\sqrt{E_2}\cos 45^{\circ} \tag{3.9}$$

Again, by substituting Eqs. (3.2)-(3.3) into Eq. (3.9) and solving for β_{eq},

$$\sqrt{\beta_{\text{eq}}} = \sqrt{2(1-\beta_{\text{eq}})}, \tag{3.10}$$

$$\beta_{\text{eq}} = \frac{2}{3}. \tag{3.11}$$

Using this result along with Eq. (3.2), the vertical boundaries along the abscissa are determined to be located at $\sqrt{\frac{2}{3}E}$ and $-\sqrt{\frac{2}{3}E}$.

The decision boundaries pose as barriers on the upper bound of β. In contrast to decreases in β, increases to the parameter cause the location of the four points s_3, s_4, s_5, and s_6 to move closer together towards their centre as more power is allocated for the base layer. Simultaneously, the centre of these four points moves further away from the origin, thus expanding the decision region of the base layer. These two movements, due to increases in β reducing $\sqrt{E_2}$ and increasing $\sqrt{E_1}$, are indicated by the arrows in Fig. 3.5. When

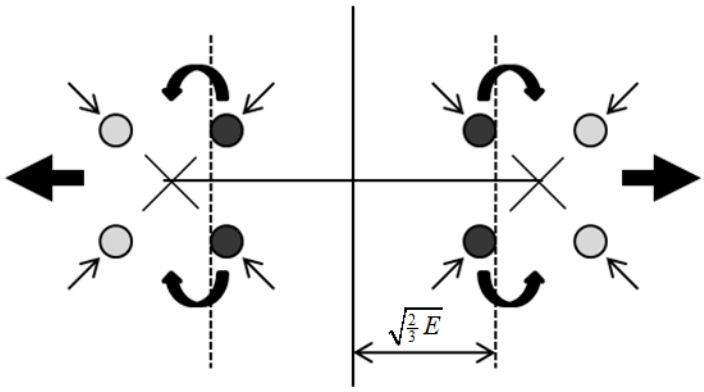

Figure 3.5: Increasing β with arrows showing directions of symbol movement.

β is increased to β_{max}, such that s_3 and s_6 cross the dashed line at $\sqrt{\frac{2}{3}E}$ on the positive abscissa of the constellation, persistent errors in distinguishing s_3 from s_4 and s_6 from s_5 would occur in the case that a standard 8-QAM demodulator is used to decode the signal.

Again, due to symmetry, the movements of s_1, s_2, s_7, and s_8 exhibits the same behaviour from variations in β with the same conditions causing s_7 and s_2 to be indistinguishable from s_8 and s_1, respectively, when using the standard 8-QAM demodulator with a decision boundary located at $-\sqrt{\frac{2}{3}E}$ on the negative abscissa.

For increasing β values, $\beta_{\max}$ occurs when the horizontal distance between any inner constellation symbol and the vertical axis approaches the width of the inner decision regions bounded between abscissa values of $-\sqrt{\frac{2}{3}E}$, 0, and $\sqrt{\frac{2}{3}E}$, eventually satisfying Eq. (3.12).

$$\sqrt{E_1} - \sqrt{\frac{E_2}{2}} = \sqrt{\frac{2}{3}E} \tag{3.12}$$

Substituting Eqs. (3.2)-(3.3) into Eq. (3.12) and numerically solving for $\beta_{\max}$,

$$\sqrt{\beta_{\max}} - \sqrt{\frac{1}{2}(1-\beta_{\max})} = \sqrt{\frac{2}{3}}, \tag{3.13}$$

$$\beta_{\max} = 0.94\dot{9}. \tag{3.14}$$

From these two subsections, it is concluded that $0.33\dot{3} < \beta < 0.94\dot{9}$ is a necessary condition for the feasibility of using a standard 8-QAM demodulator in the proposed logical SPC modulation scheme.

3.4 Design Formulations

With the same number of points in the constellation diagram, the performance of the proposed logical SPC modulation and demodulation may be different from the conventional hardware-based SPC implementation. This subsection derives expressions necessary to evaluate the symbol error rate of using the one-shot demodulator as part of the proposed logical SPC implementation of superposition coding at a receiver, as well as similar expressions for the hardware based SIC approach used by the conventional SPC implementation. Proceeding with the case study without losing generality, the analysis in this subsection is conducted using an eight point SPC constellation diagram subject to Additive White Gaussian Noise (AWGN), where receivers perform SPC demodulation based on the BPSK/QPSK combination.

The coordinates of symbol s_q can be split into the abscissa and ordinate components, which are assumed to be independent. Both components are distorted by the normally

distributed Gaussian noise with noise power $\frac{N_0}{2}$ added on top of the allocated energies E_1 and E_2. Thus, the coordinates of the eight points in the constellation diagram, $s_q : (x, x')$, are normal variables with means and variances provided in Table 3.2. The means and

Table 3.2: Mean and variance of abscissa and ordinate indicating AWGN-distorted symbol locations.

s_1 : $x \sim N\left(-\sqrt{E_1} - \sqrt{\frac{E_2}{2}}, \frac{N_0}{2}\right)$ $x' \sim N\left(+\sqrt{\frac{E_2}{2}}, \frac{N_0}{2}\right)$	s_2 : $x \sim N\left(-\sqrt{E_1} + \sqrt{\frac{E_2}{2}}, \frac{N_0}{2}\right)$ $x' \sim N\left(+\sqrt{\frac{E_2}{2}}, \frac{N_0}{2}\right)$
s_3 : $x \sim N\left(+\sqrt{E_1} - \sqrt{\frac{E_2}{2}}, \frac{N_0}{2}\right)$ $x' \sim N\left(+\sqrt{\frac{E_2}{2}}, \frac{N_0}{2}\right)$	s_4 : $x \sim N\left(+\sqrt{E_1} + \sqrt{\frac{E_2}{2}}, \frac{N_0}{2}\right)$ $x' \sim N\left(+\sqrt{\frac{E_2}{2}}, \frac{N_0}{2}\right)$
s_5 : $x \sim N\left(+\sqrt{E_1} + \sqrt{\frac{E_2}{2}}, \frac{N_0}{2}\right)$ $x' \sim N\left(-\sqrt{\frac{E_2}{2}}, \frac{N_0}{2}\right)$	s_6 : $x \sim N\left(+\sqrt{E_1} - \sqrt{\frac{E_2}{2}}, \frac{N_0}{2}\right)$ $x' \sim N\left(-\sqrt{\frac{E_2}{2}}, \frac{N_0}{2}\right)$
s_7 : $x \sim N\left(-\sqrt{E_1} + \sqrt{\frac{E_2}{2}}, \frac{N_0}{2}\right)$ $x' \sim N\left(-\sqrt{\frac{E_2}{2}}, \frac{N_0}{2}\right)$	s_8 : $x \sim N\left(-\sqrt{E_1} - \sqrt{\frac{E_2}{2}}, \frac{N_0}{2}\right)$ $x' \sim N\left(-\sqrt{\frac{E_2}{2}}, \frac{N_0}{2}\right)$

variances for each SPC symbol in Table 3.2 can be summarized as:

$$x \sim N\left(\pm\sqrt{E_1} \pm \sqrt{\frac{E_2}{2}}, \frac{N_0}{2}\right); \tag{3.15}$$

$$x' \sim N\left(\pm\sqrt{\frac{E_2}{2}}, \frac{N_0}{2}\right). \tag{3.16}$$

To account for the dependency between base and enhancement layers in successively refinable video bit streams, two symbol error expressions are necessary: base layer symbol error and compound symbol error. Base layer symbol error refers to the error probability of the base layer portion of the SPC symbol. Compound symbol error refers to the error probability of the entire SPC symbol. Recalling that L-SPC uses the one-shot standard 8-QAM demodulator and C-SPC uses the three stage process involving hardware-based SIC, the two symbol error expressions are derived in forthcoming subsections.

3.4.1 Base Layer Symbol Error

The symbol error of the base layer portion in a SPC symbol is a crucial performance metric for SPC applications in successively refinable bit streams because it is directly related to the perceived quality of the base layer, which allows further quality refinements if additional enhancement layer information can be obtained. In L-SPC, a standard 8-QAM demodulator is used, but from the strategic mapping of information bits discussed in Section 3.1.2, the base layer symbol error is equivalent to the symbol error resulting from using a BPSK demodulator. Thus, the base layer symbol error for both L-SPC and C-SPC are equal. Proceeding with the derivation of the base layer symbol error, a BPSK detector assumes that there are only two possible decisions. The decision is made based on the abscissa of the received constellation symbol. With the assumption that both base layer outcomes are equally likely to occur, the decision boundary becomes the vertical axis. Thus, the conditional base layer error probabilities, given each transmitted SPC symbol, can be individually determined and are summarized in Table 3.3.

Table 3.3: Base layer symbol error probabilities conditioned on each possible transmitted SPC symbol.

$$
\begin{array}{|l|}
\hline
P(e|s_1) = P(x > 0) = Q\left[\sqrt{\frac{2}{N_0}}\left(\sqrt{E_1} + \sqrt{\frac{E_2}{2}}\right)\right] \\
P(e|s_2) = P(x > 0) = Q\left[\sqrt{\frac{2}{N_0}}\left(\sqrt{E_1} - \sqrt{\frac{E_2}{2}}\right)\right] \\
P(e|s_3) = P(x < 0) = Q\left[\sqrt{\frac{2}{N_0}}\left(\sqrt{E_1} - \sqrt{\frac{E_2}{2}}\right)\right] \\
P(e|s_4) = P(x < 0) = Q\left[\sqrt{\frac{2}{N_0}}\left(\sqrt{E_1} + \sqrt{\frac{E_2}{2}}\right)\right] \\
P(e|s_5) = P(x < 0) = Q\left[\sqrt{\frac{2}{N_0}}\left(\sqrt{E_1} + \sqrt{\frac{E_2}{2}}\right)\right] \\
P(e|s_6) = P(x < 0) = Q\left[\sqrt{\frac{2}{N_0}}\left(\sqrt{E_1} - \sqrt{\frac{E_2}{2}}\right)\right] \\
P(e|s_7) = P(x > 0) = Q\left[\sqrt{\frac{2}{N_0}}\left(\sqrt{E_1} - \sqrt{\frac{E_2}{2}}\right)\right] \\
P(e|s_8) = P(x > 0) = Q\left[\sqrt{\frac{2}{N_0}}\left(\sqrt{E_1} + \sqrt{\frac{E_2}{2}}\right)\right] \\
\hline
\end{array}
$$

Due to symmetry in reference to Fig. 3.3, the crossover probability of the base layer, $P_{e,1}$, of all eight SPC points can be categorized into two sets of equations, expressed as:

$$
P(e|s_q) = \begin{cases} Q\left[\sqrt{\frac{2}{N_0}}\left(\sqrt{E_1} + \sqrt{\frac{E_2}{2}}\right)\right] & \text{if } q = 1, 4, 5, 8 \\ Q\left[\sqrt{\frac{2}{N_0}}\left(\sqrt{E_1} - \sqrt{\frac{E_2}{2}}\right)\right] & \text{if } q = 2, 3, 6, 7. \end{cases} \tag{3.17}
$$

With the assumption that each of the eight points are equally likely to be transmitted, the base layer SER for both L-SPC and C-SPC demodulation, denoted by $P_{2,4}^{s,1}$, can be expressed with substitutions from Eqs. (3.2)-(3.3) to result in Eq. (3.18).

$$P_{2,4}^{s,1} = \frac{1}{2}Q\left[\sqrt{\frac{2E}{N_0}}\left(\sqrt{\beta}+\sqrt{\frac{1}{2}(1-\beta)}\right)\right] + \frac{1}{2}Q\left[\sqrt{\frac{2E}{N_0}}\left(\sqrt{\beta}-\sqrt{\frac{1}{2}(1-\beta)}\right)\right] \quad (3.18)$$

3.4.2 Compound Symbol Error

The compound symbol error measures the error probability of each SPC symbol in its entirety; if any one bit is incorrect, the symbol is considered lost. For L-SPC using the standard 8-QAM one-shot demodulator, the success probability is first determined by deriving the *correctness* symbol probability of the abscissa and ordinate of transmitted symbols within each decision region. Referring back to Fig. 3.3, it is seen that for the abscissa, there are four regions of interest, each containing two distinct symbols with equal probabilities for correctly decoded abscissa components. The probabilities of correctly received abscissa components are derived as follows.

For the abscissa region containing symbols s_1 and s_8,

$$\begin{aligned} P\left(x < -\sqrt{\frac{2}{3}E} \mid s_1\right) &= P\left(x < -\sqrt{\frac{2}{3}E} \mid s_8\right) \\ &= Q\left[\sqrt{\frac{2}{N_0}}\left(\sqrt{\frac{2}{3}E} - \sqrt{E_1} - \sqrt{\frac{E_2}{2}}\right)\right]. \end{aligned} \quad (3.19)$$

For the abscissa region containing symbols s_2 and s_7,

$$\begin{aligned} &P\left(-\sqrt{\frac{2}{3}E} < x < 0 \mid s_2\right) = P\left(-\sqrt{\frac{2}{3}E} < x < 0 \mid s_7\right) \\ &= Q\left[\sqrt{\frac{2}{N_0}}\left(-\sqrt{\frac{2}{3}E} + \sqrt{E_1} - \sqrt{\frac{E_2}{2}}\right)\right] - Q\left[\sqrt{\frac{2}{N_0}}\left(\sqrt{E_1} - \sqrt{\frac{E_2}{2}}\right)\right]. \end{aligned} \quad (3.20)$$

For the abscissa region containing symbols s_3 and s_6,

$$\begin{aligned} &P\left(0 < x < \sqrt{\frac{2}{3}E} \mid s_3\right) = P\left(0 < x < \sqrt{\frac{2}{3}E} \mid s_6\right) \\ &= Q\left[\sqrt{\frac{2}{N_0}}\left(-\sqrt{\frac{2}{3}E} + \sqrt{E_1} - \sqrt{\frac{E_2}{2}}\right)\right] - Q\left[\sqrt{\frac{2}{N_0}}\left(\sqrt{E_1} - \sqrt{\frac{E_2}{2}}\right)\right]. \end{aligned} \quad (3.21)$$

For the abscissa region containing symbols s_4 and s_5,

$$P\left(x > \sqrt{\frac{2}{3}E} \mid s_4\right) = P\left(x > \sqrt{\frac{2}{3}E} \mid s_5\right)$$
$$= Q\left[\sqrt{\frac{2}{N_0}}\left(\sqrt{\frac{2}{3}E} - \sqrt{E_1} - \sqrt{\frac{E_2}{2}}\right)\right]. \tag{3.22}$$

In contrast to the abscissa, in Fig. 3.3, it is seen that for the ordinate, there are only two regions of interest, with each containing four distinct symbols with equal probabilities for correctly decoded ordinate components. The probabilities of correctly received ordinate components are derived as follows.

For the ordinate region containing symbols s_5, s_6, s_7, and s_8,

$$P\left(x' < 0 \mid s_5\right) P\left(x' < 0 \mid s_6\right) = P\left(x' < 0 \mid s_7\right) = P\left(x' < 0 \mid s_8\right) = Q\left(-\sqrt{\frac{E_2}{N_0}}\right). \tag{3.23}$$

For the ordinate region containing symbols s_1, s_2, s_3, and s_4,

$$P\left(x' > 0 \mid s_1\right) P\left(x' > 0 \mid s_2\right) = P\left(x' > 0 \mid s_3\right) = P\left(x' > 0 \mid s_4\right) = Q\left(-\sqrt{\frac{E_2}{N_0}}\right). \tag{3.24}$$

The constellation diagram is symmetric along both the abscissa and ordinate. Therefore, only symbols in the first quadrant, s_3 and s_4, need to be considered, reducing Eqs. (3.19)-(3.24) to three expressions:

$$P_0 = P\left(0 < x < \sqrt{\frac{2}{3}E} \mid s_3\right)$$
$$= Q\left[\sqrt{\frac{2}{N_0}}\left(-\sqrt{\frac{2}{3}E} + \sqrt{E_1} - \sqrt{\frac{E_2}{2}}\right)\right] - Q\left[\sqrt{\frac{2}{N_0}}\left(\sqrt{E_1} - \sqrt{\frac{E_2}{2}}\right)\right]; \tag{3.25}$$
$$P_1 = P\left(x > \sqrt{\frac{2}{3}E} \mid s_4\right)$$
$$= Q\left[\sqrt{\frac{2}{N_0}}\left(\sqrt{\frac{2}{3}E} - \sqrt{E_1} - \sqrt{\frac{E_2}{2}}\right)\right]; \tag{3.26}$$
$$P_0' = P\left(x' > 0 \mid s_3\right) = P\left(x' > 0 \mid s_4\right) = Q\left(-\sqrt{\frac{E_2}{N_0}}\right). \tag{3.27}$$

Substituting Eqs. (3.2)-(3.3) into Eqs. (3.25)-(3.27) yields:

$$P_0 = Q\left[\sqrt{\frac{2E}{N_0}}\left(-\sqrt{\frac{2}{3}}+\sqrt{\beta}-\sqrt{\frac{1}{2}(1-\beta)}\right)\right] - Q\left[\sqrt{\frac{2E}{N_0}}\left(\sqrt{\beta}-\sqrt{\frac{1}{2}(1-\beta)}\right)\right]; \tag{3.28}$$

$$P_1 = Q\left[\sqrt{\frac{2E}{N_0}}\left(\sqrt{\frac{2}{3}}-\sqrt{\beta}-\sqrt{\frac{1}{2}(1-\beta)}\right)\right]; \tag{3.29}$$

$$P_0' = Q\left(-\sqrt{\frac{E}{N_0}(1-\beta)}\right). \tag{3.30}$$

With these equations, the conditional compound symbol error probabilities, given s_3 and s_4, are derived as follows:

$$P(e|s_3) = 1 - P_0P_0'; \tag{3.31}$$

$$P(e|s_4) = 1 - P_1P_0'. \tag{3.32}$$

Finally, assuming equal transmission likelihood of each SPC symbol, the average of the individual conditional compound symbol error probabilities is the overall compound symbol error, denoted as $P_{2,4}^{s,2}$, of the one-shot demodulator designed for L-SPC.

$$P_{2,4}^{s,2} = \frac{1}{2}P(e|s_3) + \frac{1}{2}P(e|s_4) \tag{3.33}$$

$$= 1 - \frac{1}{2}(P_0P_0' + P_1P_0')$$

$$= 1 - \frac{1}{2}(P_0 + P_1)P_0' \tag{3.34}$$

Eq. (3.34) is the desired overall compound symbol error for L-SPC when a standard 8-QAM demodulator is used to decode two-layered SPC signals modulated with BPSK and QPSK. Eq. (3.34) accounts for the dependency of the two enhancement layer bits on the one base layer bit since the compound symbol error is determined based on the entirety of each SPC symbol. Thus, the received enhancement layer bits would not be considered correct unless the base layer bit is correct. Applying the same concepts to the hardware-based C-SPC demodulator, the overall compound symbol error is also determined by first deriving the correctness probability of each SPC symbol.

Both base and enhancement layers must be correctly decoded for the entire SPC symbol to be considered correct. Thus, in the first stage of conventional SPC demodulation, the BPSK detector must be successful in recovering the base layer bit and assuming a successful SIC procedure, the QPSK detector must also be successful in recovering the enhancement

layer bits. Defining B and E as respective events where the base and enhancement layers of one SPC symbol are correctly detected, the probability of both B and E occurring is equal to the correct detection of the SPC symbol. Applying the definition of conditional probability, the compound symbol error can be expressed using the intersection probability of events B and E as follows:

$$P_{2,4}^{s,2} = 1 - P(B \cap E) = 1 - P(E|B)P(B). \tag{3.35}$$

In the conventional approach, $P(E|B)$ is equal to the probability of correctly detecting the enhancement layer using a QPSK demodulator after SIC removes the BPSK energy E_1. Thus, with consideration that after SIC, the QPSK symbol only has an average of E_2 remaining, the standard symbol error equation for a QPSK demodulator is used and expressed as

$$P_{\text{QPSK}}^{s} = P(\bar{E}|B) = 2Q\left(\sqrt{\frac{E_2}{N_0}}\right) - \left[Q\left(\sqrt{\frac{E_2}{N_0}}\right)\right]^2. \tag{3.36}$$

Noting that the probability of event $\bar{B}$ occurring is intuitively the base layer symbol error as determined in the previous subsection, Eqs. (3.18) and (3.36) can be substituted into Eq. (3.35) to result in the overall compound symbol error probability, expressed in Eq. (3.37), when using the hardware-based C-SPC approach to demodulate SPC signals.

$$\begin{aligned} P_{2,4}^{s,2} &= 1 - P(E|B)P(B) \\ &= 1 - \left[1 - P(\bar{E}|B)\right]\left[1 - P(\bar{B})\right] \\ &= 1 - \left(1 - P_{\text{QPSK}}^{s}\right)\left(1 - P_{2,4}^{s,1}\right) \end{aligned} \tag{3.37}$$

Chapter 4

General Formulations

The design mechanisms of logical superposition coded modulation for mimicking a conventional BPSK/QPSK SPC modulation can be extended to any two combinations of existing modulation schemes, such as QPSK, 16-QAM, and even 64-QAM, which are adopted in current and emerging wireless standards including LTE and WiMAX. As shown in Table 3.1, any combination of modulation schemes chosen with the conventional SPC implementation with m_1 and m_2 points for the base and enhancement layers, respectively, can be theoretically decoded by a standard *one-shot* M-QAM demodulator, where $M = m_1 m_2$. This chapter's focus is to generalize the derived formulation from the previous chapter into a form applicable for any combination of two-layered SPC modulation.

4.1 Symbol Amplitude Scaling Factor

Before it is possible to derive expressions for any general two-layered SPC modulation scheme, it is necessary to first determine the symbol locations for an arbitrary c-QAM modulation. In general, for any QAM modulation, the symbols are equidistantly placed from each other and divided equally between the four quadrants in its constellation diagram. Typically, the placement of each symbol is associated with an *amplitude* scaling factor, which is necessary to normalize the average energy of the modulation scheme to unity. The symbols are placed along the odd integer multiples of the amplitude scaling factor along both the abscissa and ordinate, with the even integer multiples of the amplitude scaling factor acting as the decision boundaries for demodulation. Due to symmetry, results from the first quadrant are accurate for the entire constellation and thus, only non-

negative odd and even integer multiples need to be considered for the symbol locations and corresponding decision boundaries, respectively.

The *energy* scaling factor, used to normalize the average symbol energy to unity, is the reciprocal of the average symbol energy of a constellation diagram with symbols located at odd integers, and thus, the *amplitude* scaling factor becomes the square root of the *energy* scaling factor. The actual locations of each symbol are established by dividing the odd integers by the square root of the calculated average symbol energy to normalize the average symbol energy to unity. To proceed, the two scenarios of c-QAM constellations to consider are

$$\{c = 4^k \mid k \in \mathbb{N}_1\}, \tag{4.1}$$

$$\{c = 2 \times 4^k \mid k \in \mathbb{N}_0\}. \tag{4.2}$$

The first scenario, Eq. (4.1), refers to c-QAM constellations with an equal number of points along both the abscissa and ordinate, resulting in a squared shaped constellation diagram. Under this scenario, the symbols are located at the first $\sqrt{\frac{c}{4}}$ positive odd integers along the abscissa and ordinate. As an example, the first quadrant of a 64-QAM constellation is shown in Fig. 4.1.

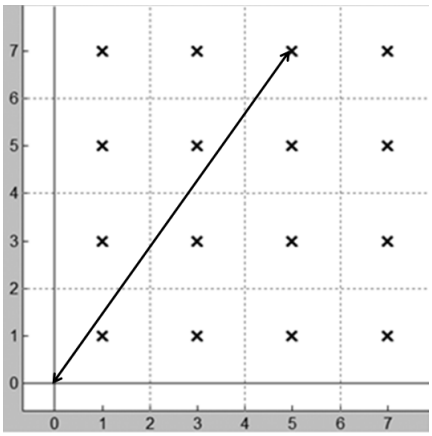

Figure 4.1: First quadrant of 64-QAM modulation scheme constellation.

In the example in Fig. 4.1, the arrow indicates the amplitude of that particular symbol. Thus, the energy of the symbol is $5^2 + 7^2$. Using the Pythagorean Theorem, the energy of each individual symbol is given by the square of each symbol's constellation amplitude. When summing the energy of all symbols, it is noted that each squared odd integer appears eight times, or $\sqrt{\frac{c}{4}}$ times for each of the two axes. Thus, for the example in Fig. 4.1, the

terms 1^2, 3^2, 5^2, and 7^2 each appear eight, or $\sqrt{\frac{c}{4}} \times 2$, times. Also, since there are always $\frac{c}{4}$ symbols in the first quadrant, the average symbol energy for the overall constellation is expressed, for the Eq. (4.1) scenario, as

$$\begin{aligned}\alpha_c &= \frac{4}{c}\left[\left(\sqrt{\frac{c}{4}} \times 2\right)\sum_{n=1}^{\sqrt{\frac{c}{4}}}(2n-1)^2\right] = \frac{4}{\sqrt{c}}\left[\sum_{n=1}^{\sqrt{\frac{c}{4}}}(2n-1)^2\right] \\ &= \frac{4}{\sqrt{c}}\left[\frac{1}{3}\left(\sqrt{\frac{c}{4}}\right)\left(2\sqrt{\frac{c}{4}}-1\right)\left(2\sqrt{\frac{c}{4}}+1\right)\right] \\ &= \frac{2}{3}(c-1). \end{aligned} \tag{4.3}$$

The second scenario, Eq. (4.2), refers to c-QAM constellations with doubled the number of points along the abscissa than the ordinate, resulting in a rectangular shaped constellation diagram. Under this scenario, the symbols are located at the first $\sqrt{\frac{c}{2}}$ and $\frac{1}{2}\sqrt{\frac{c}{2}}$ positive odd integers along the abscissa and ordinate, respectively. As an example, the first quadrant for a 32-QAM constellation is shown in Fig. 4.2.

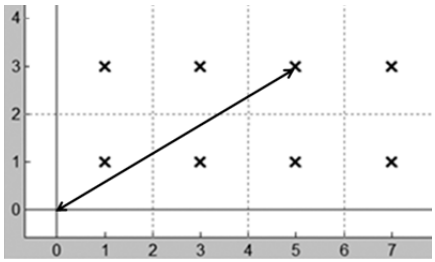

Figure 4.2: First quadrant of 32-QAM modulation scheme constellation.

In the example in Fig. 4.2, the arrow indicates the amplitude of that particular symbol. Thus, the energy of the symbol is $5^2 + 3^2$. When summing the energy of all symbols, it is noted that the first $\frac{1}{2}\sqrt{\frac{c}{2}}$ squared odd integer appears $\sqrt{\frac{c}{2}}$ times along the abscissa and $\frac{1}{2}\sqrt{\frac{c}{2}}$ along the ordinate, totalling $\frac{3}{2}\sqrt{\frac{c}{2}}$, or for the 32-QAM example, six times. However, the rest of the positive odd integers only appear $\frac{1}{2}\sqrt{\frac{c}{2}}$, or for the 32-QAM example, two times along the ordinate. Thus, for the example in Fig. 4.2, the terms 1^2 and 3^2 each appear a total of six times and the terms 5^2 and 7^2 each appear only two times. Since there are always $\frac{c}{4}$ symbols in the first quadrant, the average symbol energy for the overall

constellation is expressed, for the Eq. (4.2) scenario, as

$$\begin{aligned}
\alpha_c &= \frac{4}{c}\left[\frac{3}{2}\sqrt{\frac{c}{2}}\sum_{n=1}^{\frac{1}{2}\sqrt{\frac{c}{2}}}(2n-1)^2 + \frac{1}{2}\sqrt{\frac{c}{2}}\sum_{n=\frac{1}{2}\sqrt{\frac{c}{2}}+1}^{\sqrt{\frac{c}{2}}}(2n-1)^2\right] \\
&= \frac{4}{c}\left\{\left[\sqrt{\frac{c}{2}}\sum_{n=1}^{\frac{1}{2}\sqrt{\frac{c}{2}}}(2n-1)^2 + \frac{1}{2}\sqrt{\frac{c}{2}}\sum_{n=1}^{\frac{1}{2}\sqrt{\frac{c}{2}}}(2n-1)^2\right] + \frac{1}{2}\sqrt{\frac{c}{2}}\sum_{n=\frac{1}{2}\sqrt{\frac{c}{2}}+1}^{\sqrt{\frac{c}{2}}}(2n-1)^2\right\} \\
&= \frac{4}{c}\sqrt{\frac{c}{2}}\left[\sum_{n=1}^{\frac{1}{2}\sqrt{\frac{c}{2}}}(2n-1)^2 + \frac{1}{2}\sum_{n=1}^{\sqrt{\frac{c}{2}}}(2n-1)^2\right] \\
&= \frac{4}{c}\sqrt{\frac{c}{2}}\left[\frac{1}{3}\left(\frac{1}{2}\sqrt{\frac{c}{2}}\right)\left(\sqrt{\frac{c}{2}}-1\right)\left(\sqrt{\frac{c}{2}}+1\right) + \frac{1}{2}\times\frac{1}{3}\left(\sqrt{\frac{c}{2}}\right)\left(2\sqrt{\frac{c}{2}}-1\right)\left(2\sqrt{\frac{c}{2}}+1\right)\right] \\
&= \frac{1}{6}(5c-4). \qquad (4.4)
\end{aligned}$$

Eq. (4.5) is a summary of the average symbol energy for a c-QAM modulation scheme, based on scenarios in Eqs. (4.1)-(4.2), if symbols are placed at odd integers and decision boundaries, as a result, located at even integers. The *amplitude* scaling factor is the square root reciprocal of the average symbol energy under such assumptions, as previously discussed.

$$\alpha_c = \begin{cases} \frac{2}{3}(c-1) & \text{if } \{c = 4^k \mid k \in \mathbb{N}_1\} \\ \frac{1}{6}(5c-4) & \text{if } \{c = 2\times 4^k \mid k \in \mathbb{N}_0\} \end{cases} \qquad (4.5)$$

4.2 Formulation Scenario $\{m_1 = m_2 = 4^k \mid k \in \mathbb{N}_1\}$

This section derives the generalized formulations for the parameters previously established as necessary in evaluating the performance of logical SPC demodulation. Expressions for both base layer symbol error and compound symbol error are obtained for the scenario in Eq. (4.1), corresponding to modulation choices resulting in square shaped constellation diagrams. This section first presents formulations to represent the positions and variances of each AWGN-distorted symbol in the constellation diagram based on the power allocation parameter, β, and SNR, $\gamma = \frac{E}{N_0}$, where E is the total energy available to the SPC symbol with allocation between the two layers governed by Eqs. (3.2)-(3.3). The symbol representation equations are used to determine the probability that each received symbol occurs within its corresponding correct decision boundaries when being subject to AWGN noise. Since the abscissa and ordinate components of the noise are uncorrelated, the error

probability for each axis of any symbol can be determined independently. Due to symmetry along both the abscissa and ordinate, only one quadrant of the constellation needs to be considered.

4.2.1 Symbol Representation

Symbol locations are dependent not only on the total available energy, but also on the energy allocation between the two layers. All constellation points grow further from the origin as the total energy is increased and when the energy allocation parameter, β, is varied, the structure of the constellation points can vastly change. Recalling that each SPC symbol's constellation placement is the vector addition of the corresponding constellations from the base and enhancement layer symbols, it becomes intuitive that the placement of each generalized SPC symbol is a function of E_1 and E_2, which are energies allocated for the base and enhancement layers, respectively. To separate the entire constellation into decision regions for strictly 4^k-QAM modulation schemes with positive integer k, the abscissa and ordinate of the first quadrant in the constellation diagram can each be divided into $\sqrt{\frac{M}{4}}$ regions and referenced respectively by i and j as introduced in the equidistant QPSK/16-QAM example in Fig. 4.3.

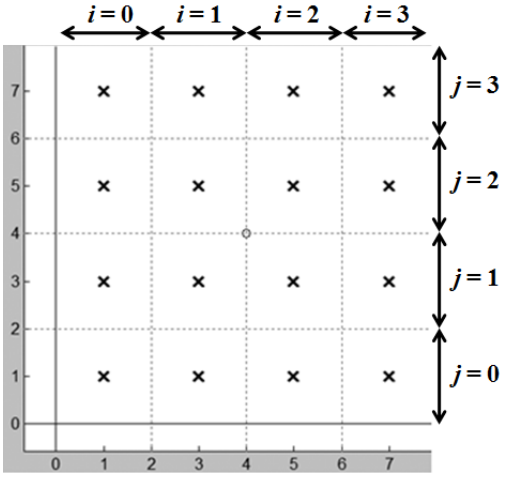

Figure 4.3: First quadrant of equidistant SPC constellation with QPSK/16-QAM combination denoting reference to each abscissa and ordinate decision region.

The variables i and j can each take non-negative integer values less than $\sqrt{\frac{M}{4}}$ such that

$$\{i, j \in \mathbb{N}_0 \mid i, j < \sqrt{\frac{M}{4}}\}. \tag{4.6}$$

Each combination of i and j refers to a specific region and the corresponding symbol, (x_i, x'_j), in the constellation diagram. The abscissa becomes represented by x_i and the ordinate by x'_j. For a two-layered SPC signal, both the abscissa and ordinate components become a linear combination of E_1 and E_2, corresponding to the energy available for the two layers. For the abscissa, $z_1(i)$ and $z_2(i)$ are expressions that relate region i, and the $\sqrt{\frac{M}{4}}$ SPC symbols within, to the corresponding odd coefficients from the base and enhancement symbol locations, respectively. Similarly for the ordinate, $z'_1(j)$ and $z'_2(j)$ are expressions that relate region j, and the $\sqrt{\frac{M}{4}}$ SPC symbols within, to the corresponding odd coefficients from the base and enhancement symbol locations, respectively. The expressions to generate the four coefficients are summarized in Eqs. (4.7)-(4.10).

$$z_1(i) = 2\left\lfloor \frac{i}{\sqrt{m_2}} \right\rfloor + 1 \tag{4.7}$$

$$z_2(i) = 2(i \bmod \sqrt{m_2}) - \sqrt{m_2} + 1 \tag{4.8}$$

$$z'_1(j) = 2\left\lfloor \frac{j}{\sqrt{m_2}} \right\rfloor + 1 \tag{4.9}$$

$$z'_2(j) = 2(j \bmod \sqrt{m_2}) - \sqrt{m_2} + 1 \tag{4.10}$$

Note that due to symmetry along the constellation diagonal,

$$z_1(j) = z'_1(j),$$

$$z_2(j) = z'_2(j).$$

Using the coefficient expressions above and letting x_i and x'_j be random variables corresponding to the abscissa and ordinate positions of the specific symbol in region i and j, the positions become normal random variables due to AWGN noise, with means and variances generalized in Eqs. (4.11)-(4.12).

$$x_i \sim N(\mu_{x_i}, \sigma_x^2) = N\left(z_1(i)\sqrt{\frac{E_1}{\alpha_{m_1}}} + z_2(i)\sqrt{\frac{E_2}{\alpha_{m_2}}}, \frac{N_0}{2} \right) \tag{4.11}$$

$$x'_j \sim N(\mu_{x'_j}, \sigma_x^2) = N\left(z'_1(j)\sqrt{\frac{E_1}{\alpha_{m_1}}} + z'_2(j)\sqrt{\frac{E_2}{\alpha_{m_2}}}, \frac{N_0}{2} \right) \tag{4.12}$$

The amplitude scaling factors, $\frac{1}{\sqrt{\alpha_c}}$, used in Eqs. (4.11) and (4.12) are multiplied by $\sqrt{E_1}$ and $\sqrt{E_2}$ to normalize the total energy available for the base and enhancement layers to E_1 and E_2, respectively, instead of unity in the previous section. Note that due to symmetry

along both the abscissa and ordinate, $x_i = x_j = x'_j$ for $i = j$.

For further simplification, define y_i and y'_j such that

$$y_i = \sqrt{\frac{\alpha_M}{E}} x_i, \tag{4.13}$$

$$y'_j = \sqrt{\frac{\alpha_M}{E}} x'_j. \tag{4.14}$$

The means and variances for y_i and y'_j can be expressed in terms of those for x_i and x'_j using the probability theorems

$$\mathbb{E}(y) = \sqrt{\frac{\alpha_M}{E}} \mathbb{E}(x), \tag{4.15}$$

$$\mathrm{Var}(y) = \frac{\alpha_M}{E} \mathrm{Var}(x), \tag{4.16}$$

and Eqs. (3.2)-(3.3) to result in

$$y_i \sim N(\mu_{y_i}, \sigma_y^2) = N\left(z_1(i)\sqrt{\frac{\beta(M-1)}{(m_1-1)}} + z_2(i)\sqrt{\frac{(1-\beta)(M-1)}{(m_2-1)}}, \frac{M-1}{3\gamma} \right), \tag{4.17}$$

$$y'_j \sim N(\mu_{y'_j}, \sigma_y^2) = N\left(z'_1(j)\sqrt{\frac{\beta(M-1)}{(m_1-1)}} + z'_2(j)\sqrt{\frac{(1-\beta)(M-1)}{(m_2-1)}}, \frac{M-1}{3\gamma} \right), \tag{4.18}$$

where

$$\sigma_y^2 = \frac{\alpha_M}{E}\sigma_x^2 = \frac{\frac{2}{3}(M-1)}{E}\frac{N_0}{2} = \frac{M-1}{3\gamma} \text{ using Eq. (4.5)}, \tag{4.19}$$

$$\gamma = \frac{E}{N_0}, \tag{4.20}$$

$$M = m_1 m_2. \tag{4.21}$$

Note that $y_i = y_j = y'_j$ for $i = j$.

4.2.2 Compound Symbol Error

The compound symbol error is determined first because its generalized form better illustrates the derivation methodology in determining a closed form expression. Compound symbol error refers to the overall symbol error probability of the entire SPC symbol. Thus, each symbol in the constellation is analyzed based on the L-SPC receiver design in using

a standard one-shot M-QAM detector to demodulate the SPC symbol. Using the generalized characteristics for each symbol representation, the compound symbol error probability can be determined using probability theory since both abscissa and ordinate components are normal variables with known derived expected values and variances. As established in Section 4.1, symbol positions of the M-QAM modulation scheme are located at *odd* integer multiples of the amplitude scaling factor, while their corresponding decision boundaries are located at *even* integer multiples of the amplitude scaling factor. Thus, again focused only on the first quadrant due to symmetry, the decision boundaries are located at $2i\sqrt{\frac{E}{\alpha_M}}$ for i values previously established as non-negative integer values less than $\sqrt{\frac{M}{4}}$. The amplitude scaling factor is multiplied by $\sqrt{E}$ to normalize the average symbol energy to E for the M-QAM modulation scheme.

Starting with the abscissa, which is divided into $\sqrt{\frac{M}{4}}$ regions, the correctness probability of a symbol's abscissa component originating from the i^{th} region is expressed as follows:

$$P_i = \begin{cases} P\left[2i\sqrt{\frac{E}{\alpha_M}} < x_i < 2(i+1)\sqrt{\frac{E}{\alpha_M}}\right] & i = 0, 1, 2, ..., \sqrt{\frac{M}{4}} - 2 \\ P\left[2i\sqrt{\frac{E}{\alpha_M}} < x_i < \infty\right] & i = \sqrt{\frac{M}{4}} - 1. \end{cases} \tag{4.22}$$

Incorporating Eq. (4.13) into Eq. (4.22) results in

$$P_i = \begin{cases} P\left[2i < y_i < 2(i+1)\right] & i = 0, 1, 2, ..., \sqrt{\frac{M}{4}} - 2 \\ P\left[2i < y_i < \infty\right] & i = \sqrt{\frac{M}{4}} - 1 \end{cases} \tag{4.23}$$

$$= \begin{cases} Q\left(\frac{2i-\mu_{y_i}}{\sigma_y}\right) - Q\left(\frac{2(i+1)-\mu_{y_i}}{\sigma_y}\right) & i = 0, 1, 2, ..., \sqrt{\frac{M}{4}} - 2 \\ Q\left(\frac{2i-\mu_{y_i}}{\sigma_y}\right) & i = \sqrt{\frac{M}{4}} - 1. \end{cases} \tag{4.24}$$

Continuing with the ordinate, which is also divided into $\sqrt{\frac{M}{4}}$ regions, the correctness probability of a symbol's ordinate component originating from the j^{th} region is expressed as follows:

$$P'_j = \begin{cases} P\left[2j\sqrt{\frac{E}{\alpha_M}} < x'_j < 2(j+1)\sqrt{\frac{E}{\alpha_M}}\right] & j = 0, 1, 2, ..., \sqrt{\frac{M}{4}} - 2 \\ P\left[2j\sqrt{\frac{E}{\alpha_M}} < x'_j < \infty\right] & j = \sqrt{\frac{M}{4}} - 1. \end{cases} \tag{4.25}$$

Incorporating Eq. (4.14) into Eq. (4.25) results in

$$P'_j = \begin{cases} P\left[2j < y'_j < 2(j+1)\right] & j = 0, 1, 2, ..., \sqrt{\frac{M}{4}} - 2 \\ P\left[2j < y'_j < \infty\right] & j = \sqrt{\frac{M}{4}} - 1 \end{cases} \tag{4.26}$$

$$= \begin{cases} Q\left(\frac{2j - \mu_{y'_j}}{\sigma_y}\right) - Q\left(\frac{2(j+1) - \mu_{y'_j}}{\sigma_y}\right) & j = 0, 1, 2, ..., \sqrt{\frac{M}{4}} - 2 \\ Q\left(\frac{2j - \mu_{y'_j}}{\sigma_y}\right) & j = \sqrt{\frac{M}{4}} - 1. \end{cases} \tag{4.27}$$

Note that $P_i = P_j = P'_j$ since $\mu_{y_i} = \mu_{y_j} = \mu_{y'_j}$ for $i = j$.

With P_i and P'_j defined as the probability of correctly decoding the respective abscissa and ordinate components of a SPC symbol in region i and j, the correctness probability of such symbol is given by the product $P_i P'_j$. Since there are $\frac{M}{4}$ symbols in the first quadrant, the average probability for correctly receiving the SPC symbol is expressed as

$$P^{c,2}_{m_1,m_2} = \frac{4}{M} \sum_{i,j} P_i P'_j \tag{4.28}$$

$$= \frac{4}{M} \left(\sum_{i=0}^{\sqrt{\frac{M}{4}}-1} P_i \right) \left(\sum_{j=0}^{\sqrt{\frac{M}{4}}-1} P'_j \right)$$

$$= \frac{4}{M} \left(\sum_{i=0}^{\sqrt{\frac{M}{4}}-1} P_i \right) \left(\sum_{j=0}^{\sqrt{\frac{M}{4}}-1} P_j \right)$$

$$= \frac{4}{M} \left(\sum_{i=0}^{\sqrt{\frac{M}{4}}-1} P_i \right)^2 . \tag{4.29}$$

The complementary probability of Eq. (4.29) is the compound symbol error probability for L-SPC, and is given by

$$P^{s,2}_{m_1,m_2} = 1 - P^{c,2}_{m_1,m_2} \tag{4.30}$$

$$= 1 - \frac{4}{M} \left(\sum_{i=0}^{\sqrt{\frac{M}{4}}-1} P_i \right)^2 . \tag{4.31}$$

As for the compound symbol error probability when using C-SPC, the method used in Section 3.4.2 can be applied again. Thus, Eq. (3.35) is applicable for any m_1 and m_2

combination for the respective base and enhancement layer modulation choices and thus, can be generalized as follows:

$$P^{s,2}_{m_1,m_2} = 1 - P(B \cap E) = 1 - P(E|B)P(B), \tag{4.32}$$

where B and E are respective events where the base and enhancement layers of one SPC symbol are correctly detected. The probability of both B and E occurring, as a result, is equal to the correct detection of the SPC symbol.

In the conventional approach, $P(E|B)$ is equal to the probability of correctly detecting the enhancement layer using a m_2-QAM demodulator after SIC removes the m_1-QAM energy E_1. Thus, with consideration that after SIC, the m_2-QAM symbol only has an average energy of E_2 remaining, the standard symbol error equation for m_2-QAM is used and expressed as

$$\begin{aligned} P^{s}_{m_2\text{-QAM}} = P(\bar{E}|B) &= 2\left[2\left(1-\frac{1}{\sqrt{m}_2}\right)Q\left(\sqrt{\frac{3}{m_2-1}\frac{E_2}{N_0}}\right)\right] \\ &\quad - \left[2\left(1-\frac{1}{\sqrt{m}_2}\right)Q\left(\sqrt{\frac{3}{m_2-1}\frac{E_2}{N_0}}\right)\right]^2 \qquad (4.33) \\ &= 2\left[2\left(1-\frac{1}{\sqrt{m}_2}\right)Q\left(\sqrt{3\gamma\frac{1-\beta}{m_2-1}}\right)\right] \\ &\quad - \left[2\left(1-\frac{1}{\sqrt{m}_2}\right)Q\left(\sqrt{3\gamma\frac{1-\beta}{m_2-1}}\right)\right]^2, \qquad (4.34) \end{aligned}$$

with substitutions from Eqs. (3.3) and (4.20).

Once again, the probability of event $\bar{B}$ occurring is intuitively the base layer symbol error, $P^{s,1}_{m_1,m_2}$, which will be derived in the generalized form in the next subsection. Eq. (4.34) can be substituted into Eq. (4.32) to result in the overall compound symbol error probability, expressed in Eq. (4.35), when using the hardware-based C-SPC approach to demodulate SPC signals.

$$\begin{aligned} P^{s,2}_{m_1,m_2} &= 1 - P(E|B)P(B) \\ &= 1 - \left[1 - P(\bar{E}|B)\right]\left[1 - P(\bar{B})\right] \\ &= 1 - \left(1 - P^{s}_{m_2\text{-QAM}}\right)\left(1 - P^{s,1}_{m_1,m_2}\right) \qquad (4.35) \end{aligned}$$

4.2.3 Base Layer Symbol Error

For base layer symbol error, the goal is to first find the probability that each received SPC symbol falls within the base layer decision boundaries. Each of the base layer decision regions are further divided into enhancement layer decision regions for each SPC symbol. Thus, it is intuitive that the base layer symbol error must always be lower than the compound symbol error since the base layer decision regions are much larger than the individual regions for each SPC symbol. The complement of the average correctness probabilities for each SPC symbol within their base layer regions becomes the base layer symbol error, which is equal between both L-SPC and C-SPC implementations because of the strategic mapping of information bits to each SPC symbol, as discussed in Sections 3.1.2 and 3.4.1.

Geometrically, each base layer decision region is divided into m_2 enhancement layer decision regions. As a result, the decision boundaries along both the abscissa and ordinate are $\sqrt{m_2}$ times larger, becoming located at even integer multiples of the product between $\sqrt{m_2}$ and the amplitude scaling factor to normalize the average symbol energy of the M-QAM constellation to E. The error probability of the base layer portion of each SPC symbol becomes dependent on the enlarged decision regions.

Beginning with the abscissa, which is divided into $\sqrt{\frac{m_1}{4}}$ base layer regions in the first quadrant, the probability of correctly decoding the abscissa component of the SPC symbol's base layer portion originating from the i^{th} region is expressed as

$$P_{i,1} = \begin{cases} P\left[2\sqrt{m_2}\left\lfloor\frac{i}{\sqrt{m_2}}\right\rfloor < y_i < 2\sqrt{m_2}\left(\left\lfloor\frac{i}{\sqrt{m_2}}\right\rfloor + 1\right)\right] & i = 0, 1, ..., \sqrt{\frac{M}{4}} - \sqrt{m_2} - 1 \\ P\left[2\sqrt{m_2}\left\lfloor\frac{i}{\sqrt{m_2}}\right\rfloor < y_i < \infty\right] & i = \sqrt{\frac{M}{4}} - \sqrt{m_2}, ..., \sqrt{\frac{M}{4}} - 1 \end{cases} \tag{4.36}$$

$$= \begin{cases} Q\left(\frac{2\sqrt{m_2}\left\lfloor\frac{i}{\sqrt{m_2}}\right\rfloor - \mu_{y_i}}{\sigma_y}\right) - Q\left(\frac{2\sqrt{m_2}\left(\left\lfloor\frac{i}{\sqrt{m_2}}\right\rfloor + 1\right) - \mu_{y_i}}{\sigma_y}\right) & i = 0, 1, ..., \sqrt{\frac{M}{4}} - \sqrt{m_2} - 1 \\ Q\left(\frac{2\sqrt{m_2}\left\lfloor\frac{i}{\sqrt{m_2}}\right\rfloor - \mu_{y_i}}{\sigma_y}\right) & i = \sqrt{\frac{M}{4}} - \sqrt{m_2}, ..., \sqrt{\frac{M}{4}} - 1. \end{cases} \tag{4.37}$$

Continuing with the ordinate, which is also divided into $\sqrt{\frac{m_1}{4}}$ base layer regions in the first quadrant, the probability of correctly decoding the ordinate component of the SPC

symbol's base layer portion originating from the j^{th} region is expressed as

$$P'_{j,1} = \begin{cases} P\left[2\sqrt{m_2}\left\lfloor \frac{j}{\sqrt{m_2}} \right\rfloor < y'_j < 2\sqrt{m_2}\left(\left\lfloor \frac{j}{\sqrt{m_2}} \right\rfloor + 1\right)\right] & j = 0, 1, ..., \sqrt{\frac{M}{4}} - \sqrt{m_2} - 1 \\ P\left[2\sqrt{m_2}\left\lfloor \frac{j}{\sqrt{m_2}} \right\rfloor < y'_j < \infty\right] & j = \sqrt{\frac{M}{4}} - \sqrt{m_2}, ..., \sqrt{\frac{M}{4}} - 1 \end{cases} \tag{4.38}$$

$$= \begin{cases} Q\left(\frac{2\sqrt{m_2}\left\lfloor \frac{j}{\sqrt{m_2}} \right\rfloor - \mu_{y'_j}}{\sigma_y}\right) - Q\left(\frac{2\sqrt{m_2}\left(\left\lfloor \frac{j}{\sqrt{m_2}} \right\rfloor + 1\right) - \mu_{y'_j}}{\sigma_y}\right) & j = 0, 1, ..., \sqrt{\frac{M}{4}} - \sqrt{m_2} - 1 \\ Q\left(\frac{2\sqrt{m_2}\left\lfloor \frac{j}{\sqrt{m_2}} \right\rfloor - \mu_{y'_j}}{\sigma_y}\right) & j = \sqrt{\frac{M}{4}} - \sqrt{m_2}, ..., \sqrt{\frac{M}{4}} - 1. \end{cases} \tag{4.39}$$

Note that $P_{i,1} = P_{j,1} = P'_{j,1}$ since $\mu_{y_i} = \mu_{y_j} = \mu_{y'_j}$ for $i = j$.

With $P_{i,1}$ and $P'_{j,1}$ defined as the probability that the respective abscissa and ordinate components of the SPC symbol, located in region i and j, is found inside its correct corresponding base layer decision region, the correctness probability of the base layer portion for each SPC symbol is given by the product $P_{i,1}P'_{j,1}$. Since there are $\frac{M}{4}$ symbols in the first quadrant, the average probability for receiving the correct base layer portion of all SPC symbols is expressed as

$$P^{c,1}_{m_1,m_2} = \frac{4}{M}\sum_{i,j} P_{i,1}P'_{j,1} \tag{4.40}$$

$$= \frac{4}{M}\left(\sum_{i=0}^{\sqrt{\frac{M}{4}}-1} P_{i,1}\right)\left(\sum_{j=0}^{\sqrt{\frac{M}{4}}-1} P'_{j,1}\right)$$

$$= \frac{4}{M}\left(\sum_{i=0}^{\sqrt{\frac{M}{4}}-1} P_{i,1}\right)\left(\sum_{j=0}^{\sqrt{\frac{M}{4}}-1} P_{j,1}\right)$$

$$= \frac{4}{M}\left(\sum_{i=0}^{\sqrt{\frac{M}{4}}-1} P_{i,1}\right)^2. \tag{4.41}$$

The complementary probability of Eq. (4.41) is the average base layer symbol error prob-

ability for both L-SPC and C-SPC, given by

$$P_{m_1,m_2}^{s,1} = 1 - P_{m_1,m_2}^{c,1} \tag{4.42}$$

$$= 1 - \frac{4}{M}\left(\sum_{i=0}^{\sqrt{\frac{M}{4}}-1} P_{i,1}\right)^2. \tag{4.43}$$

4.2.4 General Operational Range

Similar to the case study of using an one-shot 8-QAM standard demodulator to decode SPC symbols in the previous chapter, there exist lower and upper bounds for β, which are derived by identifying situations where any one of the M points in the SPC constellation occurs outside the correct decision boundaries of a standard M-QAM demodulator when the noise power is zero.

The abscissa regions are divided into groups of $\sqrt{m_2}$ to correspond to each SPC symbol's base layer symbol for a general combination of m_1-QAM and m_2-QAM for the base and enhancement layers, respectively. As β is varied, it is observed that the furthest group of SPC symbols from the origin incurs the most dramatic effects. As a result, the lower and upper bounds on β are derived using the lower corner symbol belonging to the furthest group of $\sqrt{m_2}$ abscissa regions. This symbol is always located inside the abscissa region $i = \sqrt{\frac{M}{4}} - \sqrt{m_2}$. For a general two-layered modulation with symbol locations modeled using $y_i = y_{\sqrt{\frac{M}{4}}-\sqrt{m_2}}$, the lower bound for β is reached when this symbol reaches the corresponding lower base layer decision boundary, located at an abscissa value of

$$2\sqrt{m_2}\left(\left\lfloor\sqrt{\frac{m_1}{4}}\right\rfloor - 1\right). \tag{4.44}$$

The upper bound for β, under the same conditions, occurs when such symbol reaches the next decision boundary after the corresponding lower base layer decision boundary, located at an abscissa value of

$$2\sqrt{m_2}\left(\left\lfloor\sqrt{\frac{m_1}{4}}\right\rfloor - 1\right) + 2. \tag{4.45}$$

Thus, the lower bound occurs when, for $i = \sqrt{\frac{M}{4}} - \sqrt{m_2}$, μ_{y_i} in Eq. (4.17) equals the

lower bound decision boundary, to satisfy

$$\left(2\left\lfloor\sqrt{\frac{m_1}{4}}\right\rfloor-1\right)\sqrt{\frac{\beta_{\min}(M-1)}{(m_1-1)}}+(1-\sqrt{m_2})\sqrt{\frac{(1-\beta_{\min})(M-1)}{(m_2-1)}}$$
$$=2\sqrt{m_2}\left(\left\lfloor\sqrt{\frac{m_1}{4}}\right\rfloor-1\right). \tag{4.46}$$

The upper bound, similarly, occurs when, for $i=\sqrt{\frac{M}{4}}-\sqrt{m_2}$, μ_{y_i} in Eq. (4.17) equals the upper bound decision boundary, to satisfy

$$\left(2\left\lfloor\sqrt{\frac{m_1}{4}}\right\rfloor-1\right)\sqrt{\frac{\beta_{\max}(M-1)}{(m_1-1)}}+(1-\sqrt{m_2})\sqrt{\frac{(1-\beta_{\max})(M-1)}{(m_2-1)}}$$
$$=2\sqrt{m_2}\left(\left\lfloor\sqrt{\frac{m_1}{4}}\right\rfloor-1\right)+2. \tag{4.47}$$

Using Eqs. (4.46)-(4.47), $\beta_{\min}$ and $\beta_{\max}$ can be numerically solved for scenarios where m_1 and m_2 satisfy Eq. (4.1).

4.3 Formulation Scenario $\{m_1=2, m_2=4^k \mid k\in\mathbb{N}_1\}$

This section derives formulations for the parameters previously established as necessary in evaluating the performance of logical SPC demodulation when the base layer choice is BPSK. This special scenario is considered because using BPSK as the base layer causes the overall SPC constellation to become rectangular in shape and thus, requires new expressions for symbol representation. Continuing with the previous assumptions of using AWGN-distorted SPC symbols, the expressions derived in this section are applicable only for the situation when the two-symbol BPSK modulation scheme is chosen for the base layer and any higher order 4^k-QAM modulation scheme, for positive integer k, chosen for the enhancement layer. Expressions for both the base layer and compound symbol errors are obtained for this scenario, beginning with the presentation of formulations to represent the positions and variances of each AWGN-distorted symbol in the constellation diagram based on the power allocation parameter, β, and SNR, $\gamma=\frac{E}{N_0}$, where E is the total energy available to the SPC symbol with allocation between the two layers governed by Eqs. (3.2)-(3.3). The symbol representation equations are used to determine the probability that each received symbol occurs within its corresponding correct decision boundaries when being subject to AWGN noise. Since the abscissa and ordinate components of the noise are uncorrelated, the error probability for each axis of any symbol can be determined

independently. Due to symmetry along both the abscissa and ordinate, only one quadrant of the constellation needs to be considered.

4.3.1 Symbol Representation

The symbol locations for this scenario are still dependent, not only on the total energy available, E, but also on the energy allocation parameter, β. As a result, the placement of each generalized SPC symbol is a function of E_1 and E_2, which are energies allocated for the base and enhancement layers, respectively. In this scenario, the entire constellation is separated such that the abscissa and ordinate of the first quadrant in the constellation diagram are each divided into $\sqrt{m_2}$ and $\frac{1}{2}\sqrt{m_2}$ regions and referenced respectively by i and j, as introduced in the equidistant BPSK/16-QAM example in Fig. 4.4. The BPSK symbol is located and marked at four multiples of the amplitude scaling factor along the abscissa.

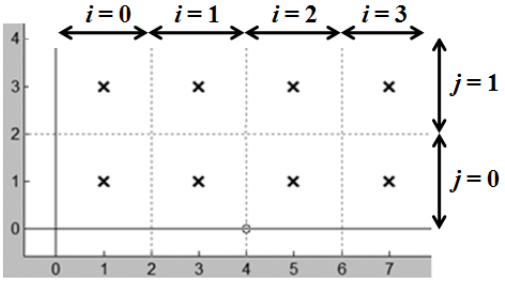

Figure 4.4: First quadrant of equidistant SPC constellation with BPSK/16-QAM combination denoting reference to each abscissa and ordinate decision region.

The variables i and j can each take non-negative integer values less than $\sqrt{m_2}$ and $\frac{1}{2}\sqrt{m_2}$, respectively, such that

$$\{i \in \mathbb{N}_0 \mid i < \sqrt{m_2}\}, \tag{4.48}$$

$$\{j \in \mathbb{N}_0 \mid j < \frac{1}{2}\sqrt{m_2}\}. \tag{4.49}$$

Each combination of i and j refers to a specific region and the corresponding symbol, (x_i, x'_j), in the constellation diagram. The abscissa becomes represented by x_i and the ordinate by x'_j. For a two-layered SPC signal, both the abscissa and ordinate components become a linear combination of E_1 and E_2, corresponding to the energy available for the two

layers. For the abscissa, $z_1(i)$ and $z_2(i)$ are expressions that relate region i, and the $\frac{1}{2}\sqrt{m_2}$ SPC symbols within, to the corresponding odd coefficients from the base and enhancement symbol locations, respectively. Similarly for the ordinate, $z'_1(j)$ and $z'_2(j)$ are expressions that relate region j, and the $\sqrt{m_2}$ SPC symbols within, to the corresponding odd coefficients from the base and enhancement symbol locations, respectively. The expressions to generate the four coefficients are summarized in Eqs. (4.50)-(4.53).

$$z_1(i) = 1 \tag{4.50}$$

$$z_2(i) = 2i - \sqrt{m_2} + 1 \tag{4.51}$$

$$z'_1(j) = 0 \tag{4.52}$$

$$z'_2(j) = 2j + 1 \tag{4.53}$$

Note that symmetry along the diagonal no longer holds for this scenario. Thus, $z_1(j) \neq z'_1(j)$ and $z_2(j) \neq z'_2(j)$.

Substituting Eqs. (4.50)-(4.53), Eqs. (4.11)-(4.12) simplifies to

$$x_i \sim N\left(z_1(i)\sqrt{\frac{E_1}{\alpha_{m_1}}} + z_2(i)\sqrt{\frac{E_2}{\alpha_{m_2}}}, \frac{N_0}{2}\right) = N\left(\sqrt{E_1} + z_2(i)\sqrt{\frac{E_2}{\alpha_{m_2}}}, \frac{N_0}{2}\right), \tag{4.54}$$

$$x'_j \sim N\left(z'_1(j)\sqrt{\frac{E_1}{\alpha_{m_1}}} + z'_2(j)\sqrt{\frac{E_2}{\alpha_{m_2}}}, \frac{N_0}{2}\right) = N\left(z'_2(j)\sqrt{\frac{E_2}{\alpha_{m_2}}}, \frac{N_0}{2}\right). \tag{4.55}$$

Using definitions in Eqs. (4.13)-(4.14) for further simplifications, the means and variances for y_i and y'_j can be expressed in terms of those for x_i and x'_j using the probability theorems in Eqs. (4.15)-(4.16) and substituting Eqs. (3.2)-(3.3), results in

$$y_i \sim N(\mu_{y_i}, \sigma^2_{y_i}) = N\left(\sqrt{\frac{\beta}{6}(5M-4)} + z_2(i)\sqrt{\frac{(1-\beta)}{4}\frac{(5M-4)}{(m_2-1)}}, \frac{5M-4}{12\gamma}\right), \tag{4.56}$$

$$y'_j \sim N(\mu_{y'_j}, \sigma^2_{y'_j}) = N\left(z'_2(j)\sqrt{\frac{(1-\beta)}{4}\frac{(5M-4)}{(m_2-1)}}, \frac{5M-4}{12\gamma}\right), \tag{4.57}$$

where

$$\sigma_y^2 = \frac{\alpha_M}{E}\sigma_x^2 = \frac{\frac{1}{6}(5M-4)}{E}\frac{N_0}{2} = \frac{5M-4}{12\gamma} \text{ using Eq. (4.5)}, \tag{4.58}$$

$$\gamma = \frac{E}{N_0}, \tag{4.59}$$

$$M = m_1 m_2 = 2m_2. \tag{4.60}$$

4.3.2 Compound Symbol Error

Similar to the derived expressions for the generalized scenario, the compound symbol error is derived in the same manner even though in this scenario, BPSK is always chosen for the base layer. The compound symbol error probability is determined using probability theory since both abscissa and ordinate components are normal variables with known expected values and variances derived in the previous subsection. As established in Section 4.1, symbol positions of the M-QAM modulation scheme are located at *odd* integer multiples of the amplitude scaling factor, while their corresponding decision boundaries are located at *even* integer multiples of the amplitude scaling factor. Along the abscissa, the decision boundaries are located at $2i\sqrt{\frac{E}{\alpha_M}}$ for i values previously established as non-negative integer values less than $\sqrt{m_2}$. Along the ordinate, the decision boundaries are located at $2j\sqrt{\frac{E}{\alpha_M}}$ for j values previously established as non-negative integer values less than $\frac{1}{2}\sqrt{m_2}$. The amplitude scaling factor is multiplied by $\sqrt{E}$ to normalize the average symbol energy to E for the M-QAM modulation scheme.

Starting with the abscissa, which is divided into $\sqrt{m_2}$ regions, the abscissa correctness probability of a symbol originating from the i^{th} region is expressed as follows:

$$P_i = \begin{cases} P\left[2i\sqrt{\frac{E}{\alpha_M}} < x_i < 2(i+1)\sqrt{\frac{E}{\alpha_M}}\right] & i = 0, 1, 2, ..., \sqrt{m_2} - 2 \\ P\left[2i\sqrt{\frac{E}{\alpha_M}} < x_i < \infty\right] & i = \sqrt{m_2} - 1. \end{cases} \tag{4.61}$$

Incorporating Eq. (4.13) into Eq. (4.61) results in

$$P_i = \begin{cases} P\left[2i < y_i < 2(i+1)\right] & i = 0, 1, 2, ..., \sqrt{m_2} - 2 \\ P\left[2i < y_i < \infty\right] & i = \sqrt{m_2} - 1 \end{cases} \tag{4.62}$$

$$= \begin{cases} Q\left(\frac{2i-\mu_{y_i}}{\sigma_y}\right) - Q\left(\frac{2(i+1)-\mu_{y_i}}{\sigma_y}\right) & i = 0, 1, 2, ..., \sqrt{m_2} - 2 \\ Q\left(\frac{2i-\mu_{y_i}}{\sigma_y}\right) & i = \sqrt{m_2} - 1. \end{cases} \tag{4.63}$$

Continuing with the ordinate, which is divided into $\frac{1}{2}\sqrt{m_2}$ regions, the ordinate correctness probability of a symbol originating from the j^{th} region is expressed as follows:

$$P'_j = \begin{cases} P\left[2j\sqrt{\frac{E}{\alpha_M}} < x'_j < 2(j+1)\sqrt{\frac{E}{\alpha_M}}\right] & j = 0, 1, 2, ..., \frac{1}{2}\sqrt{m_2} - 2 \\ P\left[2j\sqrt{\frac{E}{\alpha_M}} < x'_j < \infty\right] & j = \frac{1}{2}\sqrt{m_2} - 1. \end{cases} \tag{4.64}$$

Incorporating Eq. (4.14) into Eq. (4.64) results in

$$P'_j = \begin{cases} P\left[2j < y'_j < 2(j+1)\right] & j = 0, 1, 2, ..., \frac{1}{2}\sqrt{m_2} - 2 \\ P\left[2j < y'_j < \infty\right] & j = \frac{1}{2}\sqrt{m_2} - 1 \end{cases} \tag{4.65}$$

$$= \begin{cases} Q\left(\frac{2j - \mu_{y'_j}}{\sigma_y}\right) - Q\left(\frac{2(j+1) - \mu_{y'_j}}{\sigma_y}\right) & j = 0, 1, 2, ..., \frac{1}{2}\sqrt{m_2} - 2 \\ Q\left(\frac{2j - \mu_{y'_j}}{\sigma_y}\right) & j = \frac{1}{2}\sqrt{m_2} - 1. \end{cases} \tag{4.66}$$

With P_i and P'_j defined as the probability of correctly decoding the respective abscissa and ordinate components of a SPC symbol in region i and j, the correctness probability of such symbol is given by the product $P_i P'_j$. Since there are $\frac{M}{4}$ symbols in the first quadrant, the average probability for receiving the correct SPC symbol is expressed as

$$P^{c,2}_{2,m_2} = \frac{4}{M} \sum_{i,j} P_i P'_j \tag{4.67}$$

$$= \frac{4}{M} \left(\sum_{i=0}^{\sqrt{m_2}-1} P_i \right) \left(\sum_{j=0}^{\frac{1}{2}\sqrt{m_2}-1} P'_j \right). \tag{4.68}$$

The complementary probability of Eq. (4.68) is the compound symbol error probability for L-SPC, and is given by

$$P^{s,2}_{2,m_2} = 1 - P^{c,2}_{2,m_2} \tag{4.69}$$

$$= 1 - \frac{4}{M} \left(\sum_{i=0}^{\sqrt{m_2}-1} P_i \right) \left(\sum_{j=0}^{\frac{1}{2}\sqrt{m_2}-1} P'_j \right). \tag{4.70}$$

As for the compound symbol error probability when using C-SPC, Eq. (4.35), when using BPSK for the base layer, simplifies to

$$P^{s,2}_{2,m_2} = 1 - \left(1 - P^{s}_{m_2\text{-QAM}}\right)\left(1 - P^{s,1}_{2,m_2}\right), \tag{4.71}$$

for an arbitrary modulation choice for the enhancement layer satisfying the scenario in Eq. (4.1) with $P^{s}_{m_2\text{-QAM}}$ expressed in Eq. (4.34).

4.3.3 Base Layer Symbol Error

The base layer symbol error is again expressed by the complementary of the average correctness probabilities for each SPC symbol, which is equal between both L-SPC and C-SPC implementations because of the strategic mapping of information bits to each SPC symbol,

as discussed in Sections 3.1.2 and 3.4.1. In this scenario, where BPSK is always chosen for the base layer, it is only necessary to determine which half of the SPC constellation each SPC symbol is detected in. Thus, since BPSK is one-dimensional, the BPSK demodulator only accounts for the abscissa component of each received symbol. With focus again within the first quadrant due to symmetry along both the abscissa and ordinate, the probability of correctly detecting the abscissa of a SPC symbol in the i^{th} region is

$$P_{i,1} = P\left[0 < y_i < \infty\right] \qquad i = 0, 1, ..., \sqrt{m_2} - 1 \tag{4.72}$$

$$= Q\left(\frac{-\mu_{y_i}}{\sigma_{y_i}}\right) \qquad i = 0, 1, ..., \sqrt{m_2} - 1. \tag{4.73}$$

Since BPSK does not account for the ordinate, the correctness probability for each symbol's ordinate component is always

$$P'_{j,1} = 1, \tag{4.74}$$

regardless of which j region the SPC symbol belongs in.

With $P_{i,1}$ and $P'_{j,1}$ defined as the probability that the respective abscissa and ordinate components of the SPC symbol, located in region i and j, is found inside its correct corresponding base layer decision region, the correctness probability of the base layer portion for each SPC symbol is given by the product $P_{i,1}P'_{j,1}$. Since there are $\frac{M}{4}$ symbols in the first quadrant, the average probability for receiving the correct base layer portion of all SPC symbols is expressed as

$$P^{c,1}_{2,m_2} = \frac{4}{M}\sum_{i,j} P_{i,1}P'_{j,1} \tag{4.75}$$

$$= \frac{4}{M}\left(\sum_{i=0}^{\sqrt{m_2}-1} P_{i,1}\right)\left(\sum_{j=0}^{\frac{1}{2}\sqrt{m_2}-1} P'_{j,1}\right)$$

$$= \frac{4}{M}\left(\sum_{i=0}^{\sqrt{m_2}-1} P_{i,1}\right)\left(\frac{1}{2}\sqrt{m_2}\right)$$

$$= \frac{2\sqrt{m_2}}{M}\sum_{i=0}^{\sqrt{m_2}-1} P_{i,1}. \tag{4.76}$$

The complementary probability of Eq. (4.76) is the average base layer symbol error prob-

ability for both L-SPC and C-SPC, given by

$$P_{2,m_2}^{s,1} = 1 - P_{2,m_2}^{c,1} \tag{4.77}$$

$$= 1 - \frac{2\sqrt{m_2}}{M} \sum_{i=0}^{\sqrt{m_2}-1} P_{i,1}. \tag{4.78}$$

4.3.4 General Operational Range

Similar to the case study of using an one-shot 8-QAM standard demodulator to decode SPC symbols in the previous chapter, there exist lower and upper bounds for β, which are derived by identifying situations where any one of the M points in the SPC constellation occurs outside the correct decision boundaries of a standard M-QAM demodulator when the noise power is zero.

When BPSK is always chosen as the base layer modulation scheme, the SPC symbol most dramatically affected by variations in β is the symbol located inside the abscissa region $i = 0$. Thus, for a fixed BPSK base layer modulation and general c-QAM enhancement layer modulation satisfying Eq. (4.1), the lower bound for β is reached when this symbol, represented by y_0, reaches the corresponding lower base layer decision boundary, located at zero on the abscissa. The upper bound for β, under the same conditions, occurs when this symbol reaches the next decision boundary after the corresponding lower base layer decision boundary, located at two on the abscissa.

Thus, the lower bound occurs when, for $i = 0$, μ_{y_0} in Eq. (4.56) equals the lower bound decision boundary, to satisfy

$$\sqrt{\frac{\beta_{\min}}{6}(5M-4)} + (1-\sqrt{m_2})\sqrt{\frac{(1-\beta_{\min})}{4}\frac{(5M-4)}{(m_2-1)}} = 0. \tag{4.79}$$

Similarly, the upper bound occurs when, for $i = 0$, μ_{y_0} in Eq. (4.56) equals the upper bound decision boundary, to satisfy

$$\sqrt{\frac{\beta_{\max}}{6}(5M-4)} + (1-\sqrt{m_2})\sqrt{\frac{(1-\beta_{\max})}{4}\frac{(5M-4)}{(m_2-1)}} = 2. \tag{4.80}$$

Using Eqs. (4.79)-(4.80), $\beta_{\min}$ and $\beta_{\max}$ can be numerically solved for scenarios where m_2 satisfies Eq. (4.1) and $m_1 = 2$.

Chapter 5

Performance Evaluation

This chapter proceeds with the use of the general formulations derived in the previous chapter for two-layered SPC modulation to evaluate the system performance of L-SPC, in comparison to C-SPC, in terms of system throughput. Using system throughput, the performances of L-SPC and C-SPC are evaluated within the operational range of β under various channel conditions.

5.1 System Throughput

Symbol throughput is measured in terms of the average number of correct bits per transmission received at a receiver. Thus, as previously derived, throughput is a function of receiver SNR, $\gamma = \frac{E}{N_0}$. By taking each transmission as a symbol block, the symbol throughput of the l^{th} receiver, T_l, can be expressed as

$$
\begin{aligned}
T_l(\gamma) &= \mathbb{E}(N_B) + \mathbb{E}(N_E) && (5.1)\\
&= (\log_2 m_1)\, P^{c,1}_{m_1,m_2} + (\log_2 m_2)\, P^{c,2}_{m_1,m_2} && (5.2)\\
&= \begin{cases} (\log_2 m_1)\left(1 - P^{s,1}_{m_1,m_2}\right) + (\log_2 m_2)\left(1 - P^{s,2}_{m_1,m_2}\right) & \text{for L-SPC} \\ (\log_2 m_1)\left(1 - P^{s,1}_{m_1,m_2}\right) + (\log_2 m_2)\left(1 - P^{s}_{m_2\text{-QAM}}\right)\left(1 - P^{s,1}_{m_1,m_2}\right) & \text{for C-SPC} \end{cases} \\
&= \begin{cases} (\log_2 m_1)\left(1 - P^{s,1}_{m_1,m_2}\right) + (\log_2 m_2)\left(1 - P^{s,2}_{m_1,m_2}\right) & \text{for L-SPC} \\ \left[(\log_2 m_1) + (\log_2 m_2)\left(1 - P^{s}_{m_2\text{-QAM}}\right)\right]\left(1 - P^{s,1}_{m_1,m_2}\right) & \text{for C-SPC,} \end{cases} && (5.3)
\end{aligned}
$$

where N_B and N_E are random variables denoting the number of bits received from the base and enhancement layer bit streams, respectively. Eq. (5.3) expresses T_l for both logical SPC and conventional SPC implementations of SPC modulation, while considering the

dependency between the successively refinable data in the base and enhancement quality layers embedded in a SPC signal.

The system throughput, S_{m_1,m_2} is a summation of the throughputs for all users in the system. Denoting the total number of users in the system as N_{total}, the system throughput is thus

$$S_{m_1,m_2} = \sum_{l=1}^{N_{\text{total}}} T_l(\gamma_l), \tag{5.4}$$

where γ_l is the SNR perceived at the l^{th} receiver.

To address the issue of multi-user channel diversity, receivers are divided into two groups based on their respective instantaneous channel condition. Each group is characterized by the number of users in the group and their collective average SNR. The average SNR for each group is used to evaluate the performance of the specific group. For this purpose, a SNR threshold, denoted as γ_{th} is defined. Users experiencing poor channel conditions would have a SNR lower than γ_{th} while users experiencing good channel conditions would have a SNR greater than γ_{th}. Thus, in each of these two groups, the average SNR can be determined to be γ_{low} and γ_{high} for the low and high SNR groups, respectively. As a result, the system throughput expressed in Eq. (5.4) can be rewritten as

$$S_{m_1,m_2} = T_l(\gamma_{\text{low}}) \times N_{\text{low}} + T_l(\gamma_{\text{high}}) \times N_{\text{high}}, \tag{5.5}$$

where N_{low} and N_{high} are the number of users in the low and high SNR groups, respectively, with $N_{\text{low}} + N_{\text{high}} = N_{\text{total}}$.

5.2 System β Operational Range

As explained in Chapter 4, it is important to identify the operational range of β such that the use of an *one-shot* m_1m_2-QAM demodulator is feasible. By numerically solving for β_{min} and β_{max} using Eqs. (4.46)-(4.47) for the scenario in Section 4.2 and Eqs. (4.79)-(4.80) for the scenario in Section 4.3, the operational ranges of different combinations of modulation schemes are summarized in Table 5.1.

Table 5.1: Lower and upper bounds for β under various L-SPC combinations of modulation schemes.

Combination	$\boldsymbol{\beta_{\min}}$	$\boldsymbol{\beta_{\max}}$
BPSK/QPSK	$0.33\dot{3}$	$0.94\dot{9}$
QPSK/16-QAM	0.643	0.864
16-QAM/64-QAM	0.9234	0.9521

5.3 Numerical Results

In this section, the goal is to investigate and compare the performance of logical SPC (L-SPC) with the conventional hardware-based SPC (C-SPC) within the operational ranges of β values for each modulation combination under various channel environments. Extensive numerical experiments are conducted for evaluating the per-symbol performance as well as the overall system throughput in a wireless video multicast network. The settings of the experiments involve video bit streams with two quality layers, where three possible combinations of modulation pairs, BPSK/QPSK, QPSK/16QAM, and 16QAM/64QAM are evaluated. Both L-SPC and C-SPC are also compared with mono-modulation, denoted as MONO, which serves as a fundamental benchmark to justify the benefits of SPC modulation. MONO maintains the use of a single modulation scheme supportable by the majority of receivers.

5.3.1 System Performance with Multi-User Channel Diversity

Three scenarios are examined, where the SNR thresholds, γ_{th}, that divide the recipients into the two groups, are selected as 14 dB, 23 dB, and 31 dB, respectively. To quantify multi-user channel diversity, a number of cases to describe the histograms of multi-user channel conditions are defined, which are approximated as normal distributions with different statistical means. In addition to the histogram of the receiver channels, the behaviour of the overall system performance, S, over the operational range of β, is observed under different histograms of receiver channels.

From the results in Fig. 5.1, four observations can be made:

1. When the majority of the receivers are experiencing poor channel conditions, both

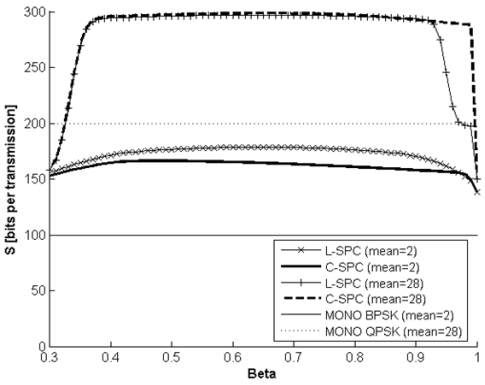

(a) BPSK/QPSK

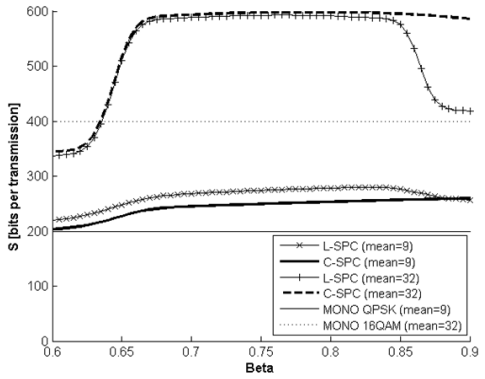

(b) QPSK/16-QAM

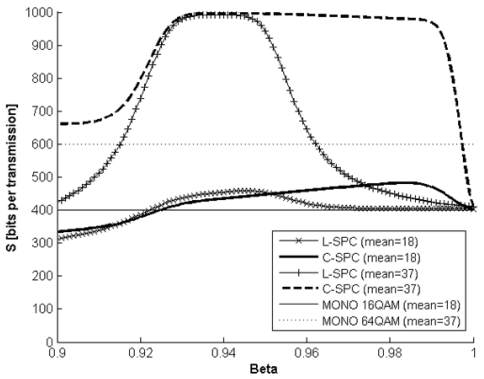

(c) 16-QAM/64-QAM

Figure 5.1: System throughput of L-SPC and C-SPC for different combinations over varying β values under normal distributions with various statistical means for SNR.

L-SPC and C-SPC perform equivalently, since most receivers are only capable of decoding the information bits from the base layer using the lower-order modulation;

2. When the statistical mean of receiver channel SNR is sufficient to support the higher order modulation in each combination, L-SPC achieves the theoretical maximum per-symbol throughput at some β value within the corresponding operational range;

3. The performance of simply using BPSK, QPSK, 16QAM alone, as indicated by the flat lines in Fig. 5.1(a)-5.1(c), respectively, are generally outperformed by L-SPC and C-SPC within the operational range of β;

4. In addition to the software implementation advantages realized in the proposed L-SPC approach, receivers equipped with the SIC-based conventional SPC technique can still be supported to demodulate the logical SPC signal with reasonable per-symbol performance for compatibility purposes.

Since SPC modulation is employed to solve the issue of multi-user channel diversity in wireless video multicast networks, it is important to evaluate its performance under different standard deviations of receiver channel distribution to characterize the diversity of multi-user channels in the entire system. Fig. 5.2 illustrates the performance of L-SPC and C-SPC for the three combinations of two-layer SPC signals of interest at low and high SNR standard deviations, yielding two sets of data for each implementation of SPC. From the results in Fig. 5.2(a)-5.2(c), two observations can be drawn:

1. For a fixed SNR mean, increased standard deviation reduces the overall system throughput due to the increase in channel diversity between the two groups of receivers;

2. For both low and high SNR standard deviation conditions, L-SPC is able to achieve comparable performance to C-SPC within the operational range of β.

With two-layer SPC signals, the SNR standard deviations should be large enough to fully demonstrate the benefits of multi-rate video transmission used by SPC signals in accommodating for the two user groups experiencing lower and higher channel SNRs. However, such SNR standard deviation should not be too large to prevent the distribution from becoming uniform. Otherwise, the SPC signal should include more than two quality layers inside the SPC signal for more multi-rates to better cater to receivers with more diverse channel conditions due to the high variance of receiver SNR.

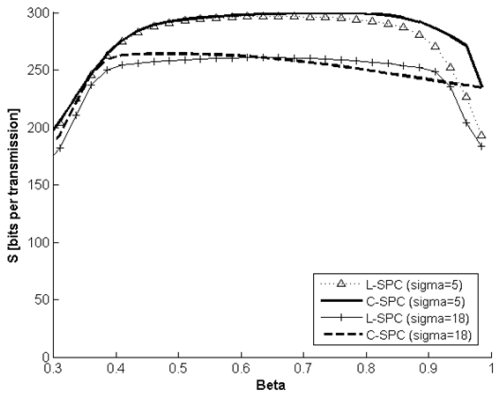

(a) BPSK/QPSK

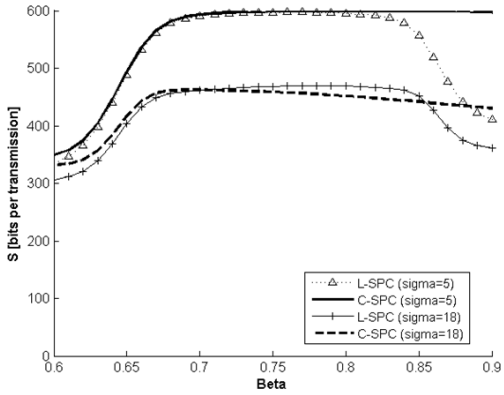

(b) QPSK/16-QAM

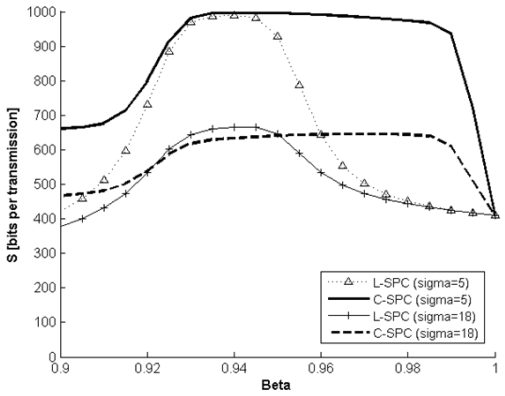

(c) 16-QAM/64-QAM

Figure 5.2: System throughput of L-SPC and C-SPC over different β values under normal distributions with various standard deviations for SNR.

5.3.2 Achieving Comparable Optimal System Performance

From the results in Fig. 5.1, it is observed that each of the C-SPC and L-SPC implementations achieve optimal system symbol throughput at different β values, which is verified over two different sets of receiver channel conditions, as well as different combinations of modulation schemes. To attain the achievable optimal system performance of the proposed approach in each multicast transmission, β should be chosen based on the given receiver channel distribution characterized by the statistical mean.

From the results in Fig. 5.3(a)-5.3(c), two conclusions can be solidly drawn:

1. L-SPC is shown to achieve comparable optimal system throughput in the wireless video multicast network for two different receiver group sizes under different average SNR values for all combinations. Both L-SPC and C-SPC are evaluated with their optimal system performances compared using β values that maximize their individual performances;

2. L-SPC, while achieving a comparable optimal system performance to C-SPC independently from the number of receivers within a wireless video multicast, also offers a much easier implementation and deployment in realizing SPC modulation and demodulation.

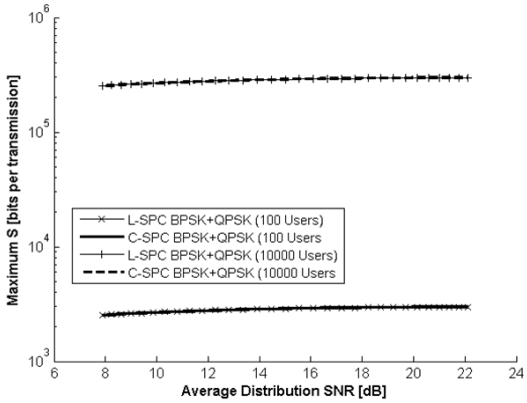

(a) BPSK/QPSK

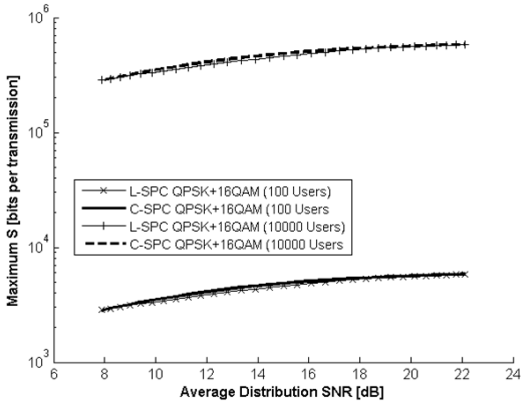

(b) QPSK/16-QAM

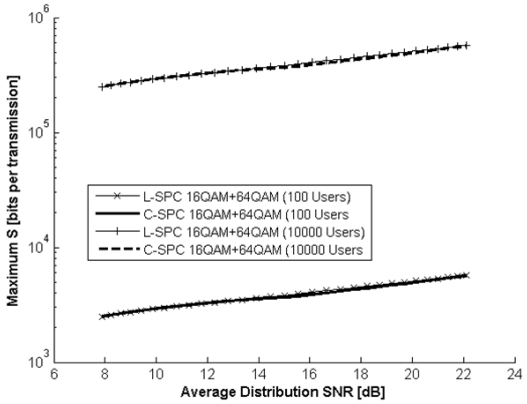

(c) 16-QAM/64-QAM

Figure 5.3: Comparable optimal system performance between L-SPC and C-SPC under different system sizes.

Chapter 6

Conclusive Remarks

Superposition coded (SPC) modulation has been well-proven as an effective approach for mitigating the vicious effect caused by multi-user channel diversity in wireless video multicasting. However, due to the requirement of additional hardware, SPC modulation and demodulation have not been commonly employed in most industry standards and practical implementations, despite the obvious advantages.

This thesis investigates a novel cross-layer design framework, known as logical SPC modulation for wireless video multicasting, which takes advantage of the successively refinable feature of scalable video bit streams. The logical SPC signals are characterized by their comparable performances under various receiver channel distributions. Rather than installing additional hardware circuitry, the proposed framework simply performs software-based dynamic energy allocation and phase keying to generate the logical SPC signals in one shot. Each receiver, on the other hand, also uses a one-shot detector to demodulate the received logical SPC signals.

Generalized formulations were derived to evaluate and analyze the proposed approach in terms of symbol error rate. Numerical simulations were conducted, and the results show that the proposed L-SPC implementation achieves better performance over mono-rate modulations in the multicast of scalable video bit streams. Also, in contrast with the conventional hardware-based SPC employing SIC, the proposed logical SPC modulation entirely avoids additional hardware at the transmitter and receivers without any compromise in the overall performance, through the manipulation of the energy allocation between the base and enhancement layers. In conclusion, the proposed logical SPC modulation not

only provides an alternative approach in realizing SPC modulation for mitigating the vicious effect of multi-user channel diversity in wireless video multicast applications, but also serves as a powerful transition tool to bridge the gap in adopting superposition coded modulation for any future wireless technologies.

Bibliography

[1] T. M. Cover, "Broadcast channels," *IEEE Trans. Information Theory*, vol. IT-18, pp. 2-14, Jan. 1972.

[2] S. Bopping et al., "Superposition coding in the downlink of CDMA cellular systems", *Proc. IEEE Wireless Communications and Networking Conference*, 2006, vol. 4, pp. 1978-1983.

[3] Chris T. K. Ng et al., "Recursive Power Allocation in Gaussian Layered Broadcast Coding with Successive Refinement," *Proc. IEEE International Conference on Communications (ICC)*, 2007, pp. 889-896.

[4] C. Tian et al., "Successive Refinement Via Broadcast: Optimizing Expected Distortion of a Gaussian Source Over a Gaussian Fading Channel," *IEEE Trans. on Information Theory*, vol. 54, no. 7, pp. 2903-2918, Jul. 2008.

[5] Y. S. Chan, et al, "An End-to-End Embedded Approach for Multicast/Broadcast of Scalable Video over Multiuser CDMA Wireless Networks," *IEEE Trans. on Multimedia*, vol. 9, no. 3, pp. 655-667, Apr. 2007.

[6] J. She et al., "IPTV over WiMAX: Key Success Factors, Challenges, and Solutions," *IEEE Communication Magazine*, vol. 45, no. 8, pp. 87-93, Aug. 2007.

[7] J. She, Y. Xiang, P.-H. Ho, E.-H. Yang, "A cross-layer design framework for robust IPTV services over IEEE 802.16 networks," *IEEE Journal on Selected Areas in Communications*, vol. 27, no. 2, pp. 235-245, Feb. 2009.

[8] M. R. Chari et al., "FLO Physical Layer: An Overview," *IEEE Trans. on Broadcasting*, vol. 53, no. 1, pp. 145-160, Mar. 2007.

[9] Qualcomm Incorporated, "Hierarchical Coding With Multiple Antennas In A Wireless Communication System," WO/2005/032035, Patent Application, Patent Cooperation Treaty, Sep. 2004.